DOI: 10.1002/chem.200600562

Iridium(III) Silyl Alkyl and Iridacyclic Compounds Supported by 4,4′-Di-*tert*-butyl-2,2′-bipyridyl

Yiu-Keung Sau,[a] Hung-Kay Lee,[b] Ian D. Williams,[a] and Wa-Hung Leung*[a]

Abstract: Treatment of $IrCl_3{\cdot}xH_2O$ with one equivalent of 4,4′-di-*tert*-butyl-2,2′-bipyridyl (dtbpy) in *N*,*N*-dimethylformamide (dmf) afforded [$IrCl_3$(dmf)(dtbpy)] (**1**). Alkylation of **1** with Me_3SiCH_2MgCl resulted in C–Si cleavage of the Me_3SiCH_2 group and formation of the Ir^{III} silyl dialkyl compound [$Ir(CH_2SiMe_3)$(dtbpy)(Me)($SiMe_3$)] (**2**), which reacted with *t*BuNC to afford [Ir(*t*BuNC)(CH_2SiMe_3)(dtbpy)(Me)($SiMe_3$)] ([**2**(*t*BuNC)]). Reaction of **2** with phenylacetylene afforded dimeric [{Ir(C≡CPh)(dtbpy)($SiMe_3$)}$_2$(μ-C≡CPh)$_2$] (**3**), in which the bridging PhC≡C$^-$ ligands are bound to Ir in a μ-σ:π fashion. Alkylation of **1** with $PhMe_2CCH_2MgCl$ afforded the cyclometalated compound [Ir(dtbpy)($CH_2CMe_2C_6H_4$)(2-$C_6H_4CMe_3$)] (**4**), which features an agostic interaction between the Ir center and the 2-*tert*-butylphenyl ligand. The cyclic voltammogram of **4** in CH_2Cl_2 shows a reversible Ir^{IV}–Ir^{III} couple at about 0.02 V versus ferrocenium/ferrocene. Oxidation of **4** in CH_2Cl_2 with silver triflate afforded an Ir^{IV} species that exhibits an anisotropic electron paramagnetic resonance (EPR) signal in CH_2Cl_2 glass at 4 K with $g_{\parallel}=2.430$ and $g_{\perp}=2.110$. Protonation of **4** with HCl and *p*-toluenesulfonic acid (HOTs) afforded [{Ir(dtbpy)(CH_2CMe_2Ph)Cl}$_2$(μ-Cl)$_2$] (**5**) and [Ir(dtbpy)(CH_2CMe_2Ph)(OTs)$_2$] (**6**), respectively. Reaction of **5** with Li[BEt_3H] gave the cyclometalated complex [{Ir(dtbpy)($CH_2CMe_2C_6H_4$)}$_2$(μ-Cl)$_2$] (**7**). Reaction of **4** with tetracyanoethylene in refluxing toluene resulted in electrophilic substitution of the iridacycle by $C_2(CN)_3$ with formation of [Ir(dtbpy)($CH_2CMe_2C_6H_3${4-$C_2(CN)_3$})(2-$C_6H_4CMe_3$)] (**8**). Reaction of **4** with diethyl maleate in refluxing toluene gave the iridafuran compound [Ir(dtbpy)($CH_2CMe_2C_6H_4$){κ^2(*C*,*O*)-C(CO_2Et)CH(CO_2Et)}] (**9**). Treatment of **9** with 2,6-dimethylphenyl isocyanide (xylNC) led to cleavage of the iridafuran ring and formation of [Ir(dtbpy)($CH_2CMe_2C_6H_4$){C(CO_2Et)CH(CO_2-Et)}(xylNC)] (**10**). Protonation of **9** with HBF_4 afforded the dinuclear neophyl complex [(Ir(dtbpy)(CH_2CMe_2-Ph){κ^2(*C*,*O*)-C(CO_2Et)CH(CO_2Et)})$_2$]-[BF_4]$_2$ (**11**). The solid-state structures of complexes **2**–**5** and **8**–**11** have been determined.

Keywords: alkylation · bipyridyl ligands · cyclometalation · iridium · metallacycles

Introduction

Iridium compounds containing diimine ligands, notably 2,2′-bipyridyl (bpy), have attracted much attention due to their interesting luminescent properties[1,2] and their applications in organic synthesis and homogeneous catalysis.[3–6] Our interest in bpy-supported organoiridium complexes has been stimulated by recent reports that Ir(bpy) compounds can catalyze selective borylation[5] and silylation[6] of arenes and heterocyclic compounds. It is believed that the active species involved in Ir-catalyzed borylation with $B_2(pin)_2$ (pin = pinacolato) are five-coordinate [$Ir(Bpin)_3L_2$] species that activate arene C–H bonds.[6–8] Indeed, [$Ir(Bpin)_3$(coe)(dtbpy)] (coe = cyclooctene, dtbpy = 4,4′-di-*tert*-butyl-2,2′-bipyridyl), which has been isolated and structurally characterized, can facilitate the stoichiometric borylation of arenes.[4a] It seems that the electron-rich, chelating bpy ligand plays a special role in stabilizing the reactive Ir^{III} tris-boryl species and facilitates its oxidative addition to C–H bonds.[4a,5j,6a] This prompted us to explore the organometallic chemistry of Ir(bpy) alkyl complexes.

The most extensively investigated organoiridium bpy compounds are half-sandwich [Ir(bpy)Cp*L]$^{2+}$ (Cp* = η^5-C_5Me_5)[3] and cyclometalated [Ir(bpy)(NC)$_2$]$^+$ species.[9,10]

[a] Dr. Y.-K. Sau, Prof. Dr. I. D. Williams, Prof. Dr. W.-H. Leung
Department of Chemistry and Open Laboratory of Chirotechnology of the Institute of Molecular Technology for Drug Discovery and Synthesis, The Hong Kong University of Science and Technology
Clear Water Bay, Kowloon, Hong Kong (China)
Fax: (+852) 2358-1594
E-mail: chleung@ust.hk

[b] Prof. Dr. H.-K. Lee
Department of Chemistry, The Chinese University of Hong Kong
Shatin, New Territories, Hong Kong (China)

Relatively few Ir^{III}(bpy) compounds containing σ-alkyl ligands have been reported. This is in contrast to isoelectronic group 10 M^{IV}(bpy) alkyl complexes (M = Pd, Pt), which have been studied extensively due to their roles in metal-catalyzed organic reactions.[11] Of note are cationic $[Pt^{IV}(\widehat{NN})Me]^+$ complexes, which are believed to be reactive intermediates in the Pt-catalyzed activation of alkanes.[12] We are also interested in higher valent Ir(bpy) alkyl compounds because Ir^{V} alkyl intermediates are involved in the oxidative addition of Ir^{III} to C–H bonds.[6–8,13] Additionally, it has been reported that the reactivity of $[Ir^{III}Cp^*Me_2(PR_3)]$ towards arenes is greatly enhanced by oxidation of the metal center.[14] Ir^{IV} and Ir^{V} alkyls are less common than their Ir^{III} and Ir^{I} congeners. Examples of isolated Ir^{V} alkyl and aryl compounds include $[IrCp^*Me_4]$,[15] $[IrCp^*(H)(PMe_3)\{\eta^2\text{-}SiPh_2(C_6H_4)\}][B(C_6F_5)_4]$,[13d] and the mesityl compounds $[Ir(mes)_4]^+$[16] and $[Ir(mes)_3(O)]$ (mes = 2,4,6-$Me_3C_6H_2$).[17] Stable Ir^{IV} σ-alkyl compounds are rare.[14b,16]

In this paper, the synthesis and reactivity of bpy-supported Ir^{III} alkyl compounds is reported. We have found that alkylation of $[IrCl_3(dmf)(dtbpy)]$ (dmf = *N*,*N*-dimethylformamide) with Me_3SiCH_2MgCl and $PhMe_2CCH_2MgCl$ leads to C–Si bond cleavage of the CH_2SiMe_3 group and cyclometalation of the neophyl group, respectively, demonstrating some intriguing organometallic chemistry exhibited by the Ir^{III}(bpy) core. Herein, we describe the synthesis and crystal structures of Ir^{III} silyl dialkyl and iridacyclic compounds supported by dtbpy. Reactions of the dtbpy-supported iridacyclic compound with tetracyanoethylene and diethyl maleate are also reported.

Results and Discussion

Ir silyl dialkyl compound: The trichloride compound $[IrCl_3(dmf)(dtbpy)]$ (**1**), prepared by reaction of $IrCl_3{\cdot}x\,H_2O$ with one equivalent of dtbpy in dmf, was used as the starting material for Ir^{III}(bpy) alkyl compounds. Transmetalation of **1** with a variety of alkylating agents, including lithium alkyls, aluminum alkyls, and Grignard reagents, has been attempted. However, in most cases, oily materials that were found to be insoluble in hexane were isolated. Only the alkylation of **1** with Me_3SiCH_2MgCl and $PhMe_2CCH_2MgCl$ led to the isolation of crystalline products that could be characterized by using X-ray crystallography (Table 1).

Treatment of **1** with three equivalents of Me_3SiCH_2MgCl in THF afforded the Ir^{III} silyl dialkyl compound $[Ir(CH_2SiMe_3)(dtbpy)(Me)(SiMe_3)]$ (**2**) in 63% yield (Scheme 1). In contrast, alkylation of **1** with Me_3CCH_2MgCl resulted in an intractable material that did not crystallize. The ^1H NMR spectrum of **2** in C_6D_6 shows three singlets at $\delta = 0.12$, 0.33, and 2.34 ppm, attributable to the methyl protons of the CH_2SiMe_3, $SiMe_3$, and Me ligands, respectively. The methylene protons of the CH_2SiMe_3 ligand are diastereotopic and appear as two doublets at $\delta = 2.13$ and 2.47 ppm ($J = 11.7$ Hz). We were unable to observe the ^{29}Si resonance signal of the $SiMe_3$ ligand. C–Si cleavage of coordinated CH_2SiR_3 ligands to give metal silyl complexes is well precedented.[18–21] Previously, Girolami and co-workers reported that alkylation of $[\{RuCl_2Cp^*\}_2]$ with Me_3SiCH_2MgCl afforded $[Ru_2(\mu\text{-}CH_2)(\mu\text{-}Cl)(Cp^*)_2(SiMe_3)]$, which underwent a reversible C–Si bond cleavage/re-formation process.[21b,c] Therefore, it seems reasonable to propose that the formation of **2** involves C–Si cleavage of an $Ir(CH_2SiMe_3)$

Table 1. Crystallographic data and experimental details for **2**–**5** and **8**–**11**.

	2	**3**	**4**	**5**	**8**·CH_2Cl_2	**9**	**10**	**11**
formula	$C_{52}H_{94}N_4Si_4Ir_2$	$C_{74}H_{86}N_4Si_2Ir_2$	$C_{38}H_{49}N_2Ir$	$C_{56}H_{74}N_4Cl_4Ir_2$	$C_{44}H_{50}N_5Cl_2Ir$	$C_{36}H_{47}N_2O_4Ir$	$C_{45}H_{56}IrN_3O_4$	$C_{80}H_{105}N_4B_2F_8O_8Cl_4Ir_2$
M_r	1272.07	1472.05	725.99	1329.39	911.99	763.96	895.13	1950.5
a [Å]	13.512(1)	10.774(2)	10.804(7)	11.169(2)	11.818(2)	11.057(5)	12.0144(9)	112.586(8)
b [Å]	13.981(1)	21.004(4)	12.109(8)	11.864(2)	14.043(2)	18.955(8)	19.6339(14)	20.249(1)
c [Å]	18.023(1)	14.766(3)	14.661(9)	21.381(4)	15.617(3)	16.398(7)	19.9607(14)	16.896(1)
α [°]	70.083(1)	90	108.094(1)	90	114.780(3)	90	66.741(1)	90
β [°]	85.155(1)	97.687(3)	93.043(1)	95.95(3)	90.569(3)	99.344(1)	89.789(1)	95.328(1)
γ [°]	65.396(1)	90	111.881(1)	90	111.983(3)	90	82.784(1)	90
V [Å^3]	2904(4)	3312(1)	1661(2)	2818(1)	2139(6)	3391(3)	4286.1(5)	4288(5)
Z	2	2	2	2	2	4	4	2
crystal system	triclinic	monoclinic	triclinic	monoclinic	triclinic	monoclinic	triclinic	monoclinic
space group	$P\bar{1}$	$P2_1/c$	$P\bar{1}$	$P2_1/c$	$P\bar{1}$	$P2_1/c$	$P\bar{1}$	$P2_1/n$
ρ_{calcd} [g cm^{-3}]	1.455	1.476	1.452	1.567	1.416	1.496	1.387	1.511
T [K]	100(2)	100(2)	100(2)	100(2)	100(2)	100(2)	298(2)	100(2)
μ [mm^{-1}]	4.695	4.095	4.048	4.950	3.281	3.977	3.158	3.300
F(000)	1288	1480	736	1320	920	1544	1824	1962
no. of reflns	17365	18020	10240	20870	11976	16459	34521	39635
no. of independent reflns	10049	5800	7453	5473	8237	5861	14366	7465
R_{int}	0.0255	0.0936	0.0213	0.0491	0.0255	0.0229	0.0333	0.0431
$R1$, $wR2$ ($I > 2\sigma(I)$)	0.0333, 0.0722	0.0435, 0.0636	0.0333, 0.0741	0.0322, 0.0660	0.0421, 0.0880	0.0235, 0.0560	0.0291, 0.0519	0.0370, 0.0927
$R1$, $wR2$ (all data)	0.0487, 0.0765	0.0900, 0.0704	0.0401, 0.0772	0.0542, 0.0699	0.0595, 0.0929	0.0282, 0.0576	0.0507, 0.0550	0.0549, 0.0990
GoF	0.995	0.908	1.037	1.005	0.998	1.041	0.975	1.062

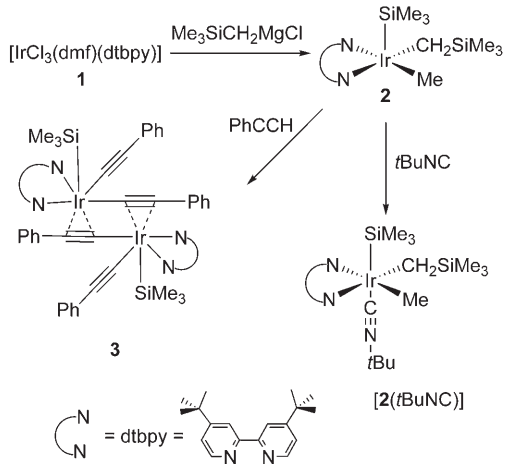

Scheme 1. Synthesis of the Ir^{III} silyl alkyl compound **2** and its reaction with phenylacetylene.

intermediate, although it is not clear how the resulting methylene species $Ir(CH_2)(SiMe_3)$ undergoes hydride transfer to give the product. Alternatively, $Ir(Me)(SiMe_3)$ may be derived from 1,2-silyl group migration of an Ir alkyl hydride intermediate, $Ir(CH_2SiMe_3)(H)$. It should be noted that silyl group migration in $[Pt(CH_2SiMe_3)(dtbpm)(H)]$ (dtbpm = bis(di-*tert*-butylphenylphosphino)methane) to give $[Pt(dtbpm)(Me)(SiMe_3)]$ has been reported by Hofmann and co-workers.[19a] Additional mechanistic studies are needed to establish the exact mechanism of the formation of **2** from **1**.

Coordinatively unsaturated **2** was found to react with two-electron ligands to give six-coordinate adducts. For example, treatment of **2** with CO afforded an oily material that exhibited a C–O band in its IR spectrum at $\tilde{\nu}$ = 2020 cm^{-1}, suggestive of the formation of the adduct [**2**(CO)]. No acyl C=O band in the region $\tilde{\nu}$ = 1600–1700 cm^{-1} was observed, indicating that the CO did not undergo insertion into an Ir–C bond. Similarly, treatment of **2** with *t*BuNC afforded $[Ir(tBuNC)(CH_2SiMe_3)(dtbpy)(Me)(SiMe_3)]$ ([**2**(*t*BuNC)]). As in the case of [**2**(CO)], the isocyanide binds to Ir without undergoing insertion into an Ir–C bond. No reactions were observed between **2** and alkenes or benzene (80 °C for 12 h). However, **2** was found to react readily with terminal alkynes such as phenylacetylene. Treatment of **2** with phenylacetylene in benzene afforded a red precipitate, which was identified as the alkynyl-bridged dimer $[\{Ir(C{\equiv}CPh)(dtbpy)(SiMe_3)\}_2(\mu\text{-}C{\equiv}CPh)_2]$ (**3**) by using X-ray crystallography. Both the methyl and trimethylsilylmethyl ligands in **2** were displaced by phenylacetylene, whereas the $SiMe_3$ group remained intact, reflecting the strong Ir^{III}–Si interaction. The conversion of **2** into the dialkynyl compound **3** involves either an oxidative addition-reductive elimination or a sigma-bond metathesis pathway. Additional mechanistic studies are required to differentiate between the two pathways. The IR spectrum of **3** shows two $\tilde{\nu}$(C≡C) bands at 2050 and 2096 cm^{-1} attributable to the terminal and bridging alkynyl ligands, respectively. We have not further explored the reactivity of **3** due to its low solubility in common organic solvents.

Complex **2** has been characterized by means of an X-ray diffraction study. The asymmetric unit contains two independent molecules. The structure of one of these molecules is shown in Figure 1; selected bond lengths and angles are listed in Table 2. The geometry around the Ir is pseudo-

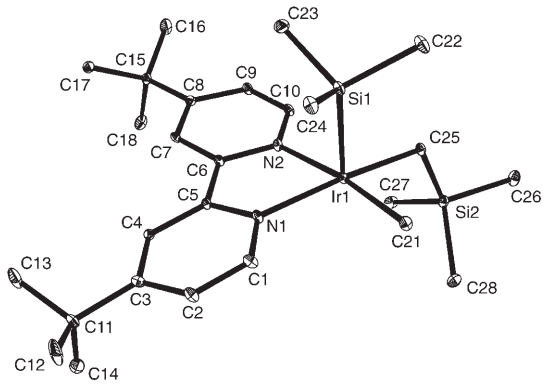

Figure 1. Molecular structure of one of the two independent molecules in the asymmetric unit of $[Ir(CH_2SiMe_3)(dtbpy)(Me)(SiMe_3)]$ (**2**). Hydrogen atoms are omitted for clarity. The ellipsoids are drawn at a 40% probability level.

Table 2. Selected bond lengths [Å] and angles [°] for $[Ir(CH_2SiMe_3)(dtbpy)(Me)(SiMe_3)]$ (**2**).

Ir1–C21	2.069(5)	Ir1–C25	2.086(5)
Ir1–N1	2.085(4)	Ir1–N2	2.096(4)
Ir1–Si1	2.279(2)	Ir2–C51	2.066(5)
Ir2–C55	2.071(5)	Ir2–N4	2.080(4)
Ir2–N3	2.103(4)	Ir2–Si3	2.272(2)
C21-Ir1-N1	96.8(2)	C21-Ir1-C25	86.9(2)
N1-Ir1-C25	170.9(2)	C21-Ir1-N2	172.8(2)
N1-Ir1-N2	76.9(2)	C25-Ir1-N2	98.84(2)
C21-Ir1-Si1	88.9(2)	N1-Ir1-Si1	93.3(1)
C25-Ir1-Si1	95.0(2)	N2-Ir1-Si1	94.8(1)
C51-Ir2-C55	88.3(2)	C51-Ir2-N4	95.7(2)
C55-Ir2-N4	170.9(2)	C51-Ir2-N3	172.0(2)
C55-Ir2-N3	98.5(2)	N4-Ir2-N3	77.0(2)
C51-Ir2-Si3	88.9(2)	C55-Ir2-Si3	92.1(1)
N4-Ir2-Si3	96.1(1)	N3-Ir2-Si3	95.0(1)

square-pyramidal, with the $SiMe_3$ group occupying the apical position, reflecting its strong *trans* influence. The Ir is displaced by about 0.127 Å above the N_2C_2 plane. No agostic interaction was found for **2**, despite its 16-electron configuration. The Ir–N distances (av. 2.091(4) Å) are similar to those in $[Ir(Br\text{-}ppy)_2(dtbpy)]^+$ (Br-ppy = 4-bromo-2-(2-pyridyl)phenyl; 2.129(9) Å).[22] The Ir–CH_3 and Ir–CH_2SiMe_3 distances (av. 2.068(5) and av. 2.079(5) Å, respectively) are typical for Ir^{III} alkyl complexes. The average Ir–Si distance of 2.276(2) Å is within the range for reported Ir^{III} silyl complexes (2.235–2.454 Å).[23]

A perspective view of **3** is shown in Figure 2; selected bond lengths and angles are listed in Table 3. The structure

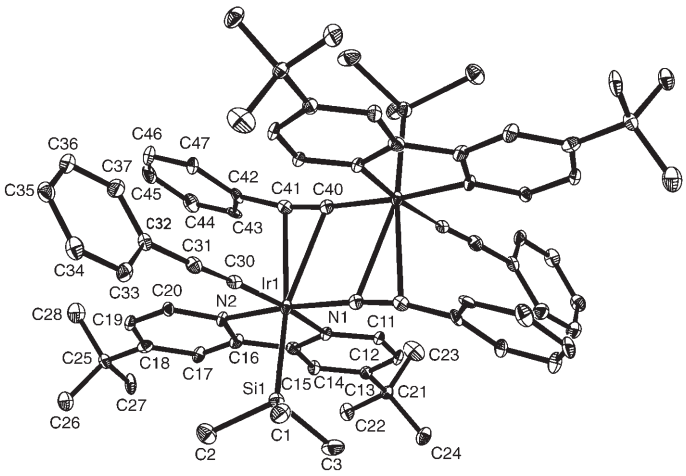

Figure 2. Molecular structure of [{Ir(C≡CPh)(dtbpy)($SiMe_3$)}$_2$(μ-C≡CPh)$_2$] (**3**). Hydrogen atoms are omitted for clarity. The ellipsoids are drawn at a 40% probability level.

Table 3. Selected bond lengths [Å] and angles [°] for [{Ir(C≡CPh)(dtbpy)($SiMe_3$)}$_2$(μ-C≡CPh)$_2$] (**3**).

Ir1–C30	1.945(6)	Ir1–C40A	1.986(7)
Ir1–N2	2.072(4)	Ir1–N1	2.082(5)
Ir1–Si1	2.331(2)	Ir1–C40	2.605(7)
Ir1–C41	2.618(7)	C40–Ir1A	1.986(7)
C30-Ir1-C40A	93.2(2)	C30-Ir1-N2	92.7(2)
C40A-Ir1-N2	173.5(2)	C30-Ir1-N1	170.6(2)
C40A-Ir1-N1	96.1(2)	N2-Ir1-N1	78.0(2)
C30-Ir1-Si1	88.4(2)	C40A-Ir1-Si1	86.7(2)
N2-Ir1-Si1	90.7(2)	C30-Ir1-C40	92.0(2)
C40A-Ir1-C40	72.7(3)	N2-Ir1-C40	109.9(2)
N1-Ir1-C40	91.3(2)	Si1-Ir1-C40	159.4(2)
C30-Ir1-C41	89.2(2)	C40A-Ir1-C41	99.4(3)
N2-Ir1-C41	83.4(2)	N1-Ir1-C41	89.7(2)
Si1-Ir1-C41	173.5(2)	C40-Ir1-C41	26.8(2)

of **3** consists of two symmetry-related [Ir(C≡CPh)(dtbpy)($SiMe_3$)]$^+$ fragments bridged by two PhC≡C$^-$ ligands that bind to the two Ir centers in a μ-σ:π fashion. In each of the fragments, the geometry about the Ir is roughly octahedral, with the $SiMe_3$ group opposite to the μ-σ:π-alkynyl ligand. The Ir–Si (2.331(2) Å) and Ir–N distances (av. 2.077(5) Å) are similar to those in **2**. The Ir–C σ-bond length in the terminal alkynyl ligand (1.945(6) Å) is slightly shorter than that in the bridging one (1.986(7) Å). In the bridging alkynyl ligands, the two Ir–C π-bond lengths (2.605(7) and 2.618(7) Å) are similar. The C≡C distance in the bridging alkynyl ligands (1.240(8) Å) is longer than that in the terminal ones (1.208(8) Å), consistent with the IR spectral data.

Iridacyclic compound 4: Treatment of **1** with three equivalents of $PhMe_2CCH_2MgCl$ led to isolation of the iridacyclic compound [Ir(dtbpy)($CH_2CMe_2C_6H_4$)(2-$C_6H_4CMe_3$)] (**4**). While group 10 metallacycles derived from bis-neophyl complexes are well known,[24] to the best of our knowledge **4** is the first example of such a metallacycle containing a group 9 metal to be characterized by X-ray crystallography. It seems reasonable to assume that the alkylation initially gave a tris-neophyl complex that underwent cyclometalation and elimination of *tert*-butylbenzene to give a mononeophyl intermediate.[25] Subsequent isomerization of the neophyl ligand, presumably by way of cyclometalation and reductive elimination, afforded the 2-*tert*-butylphenyl complex **4** (Scheme 2). It may be noted that thermal isomerization of Pd^{II}–CH_2CMe_2Ph to give Pd^{II}–C_6H_4-*o*-*t*Bu species has been reported previously by Cámpora et al.[26]

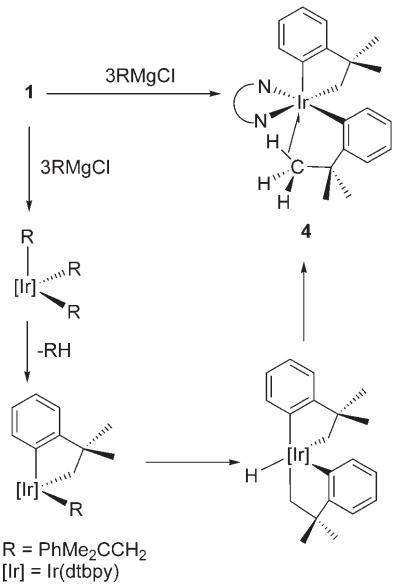

Scheme 2. Proposed mechanism for the formation of **4**.

The ^{1}H NMR spectrum of **4** was found to be solvent dependent. In C_6D_6, the diastereotopic methylene and methyl protons of the iridacycle appear as two doublets at $\delta = 3.32$ and 3.66 ppm ($J = 10.8$ Hz) and two singlets at $\delta = 1.53$ and 1.98 ppm, respectively. In $CDCl_3$, these resonances are shifted to more upfield positions ($\delta = 2.74$ (d; CH_2) and 2.94 (d; CH_2) and 0.91 ppm (Me)). Although the solid-state structure of **4** shows that there is an agostic interaction between the Ir and the 2-*tert*-butylphenyl ligand (see below), a single resonance is observed for the *tert*-butyl protons ($\delta = 0.81$ ppm) down to −50 °C in $CDCl_3$, which indicates that the three methyl groups of the 2-*tert*-butylphenyl ligand are in rapid motion about the Ir on the NMR timescale.

The molecular structure of **4** is shown in Figure 3; selected bond lengths and angles are listed in Table 4. The geometry about the Ir is pseudo-square-pyramidal, with the phenyl ring of the iridacycle occupying the apical position. A δ-agostic interaction was found between the Ir and one methyl C–H unit of the *tert*-butylphenyl ligand. The Ir···H-(agostic) and Ir–C(agostic) distances (1.91(1) and 2.649(4) Å, respectively) are similar to those in [Ir(H)$_2$(L)(PPh$_3$)$_2$]$^+$ (L = 8-methylquinoline; 2.08(10) and 2.69(1) Å, respectively).[26] In the iridacycle, the Ir–C(aryl) distance (1.990(4) Å) is shorter than the Ir–C(alkyl) distance

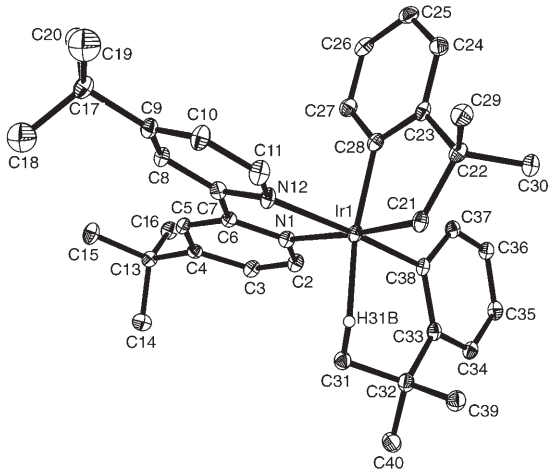

Figure 3. Molecular structure of [Ir(dtbpy)($CH_2CMe_2C_6H_4$)(2-$C_6H_4CMe_3$)] (**4**). Hydrogen atoms other than the agostic hydrogen H31B are omitted for clarity. The ellipsoids are drawn at a 40% probability level.

Table 4. Selected bond lengths [Å] and angles [°] for [Ir(dtbpy)($CH_2CMe_2C_6H_4$)(2-$C_6H_4CMe_3$)] (**4**).

Ir1–C28	1.990(4)	Ir1–C38	2.022(4)
Ir1–C21	2.073(4)	Ir1–N1	2.125(3)
Ir1–N12	2.142(3)		
C28-Ir1-C38	95.7(2)	C28-Ir1-C21	82.4(2)
C38-Ir1-C21	93.3(2)	C28-Ir1-N1	96.0(2)
C38-Ir1-N1	93.4(1)	C21-Ir1-N1	173.2(1)
C28-Ir1-N12	85.3(1)	C38-Ir1-N12	169.9(1)
C21-Ir1-N12	96.8(1)	N1-Ir1-N12	76.5(1)

(2.073(4) Å) and is comparable to that in the 2-*tert*-butylphenyl ligand (2.022(4) Å). The C-Ir-C′ angle in the iridacycle of 82.4(2)° is comparable to that in the octahedral palladia(IV)cycle [TpPd($CH_2CMe_2C_6H_4$)(NO)] (Tp = hydridotris(pyrazolyl)borate) (81.3(2)°).[27] The Ir–N distances (2.142(3) and 2.125(3) Å) are similar to those in **2**.

Protonation of 4: Complex **4** is remarkably stable in both the solid state and solutions and can be purified by means of column chromatography. It is inert towards CO, SO_2, and isocyanides, presumably because of the steric effect of the bulky 2-*tert*-butylphenyl ligand. No reactions were observed between **4** and alkenes or alkynes. Prolonged heating of **4** in benzene for 12 h yielded an uncharacterized brown material along with unreacted **4**. Previously, Cámpora et al. have reported that protonation of palladacycles affords Pd–CH_2CMe_2Ph, in which the Pd is stabilized by a π,η^1-interaction with the *ipso*-carbon atom of the phenyl ring.[25,28] This prompted us to study the reactions of **4** with acids. Treatment of **4** with triflic acid resulted in an intractable material that has yet to be characterized. Protonation of **4** with HCl in Et_2O resulted in the precipitation of a red solid characterized as the chloro-bridged dimer [{Ir(dtbpy)(CH_2CMe_2Ph)Cl}$_2$(μ-Cl)$_2$] (**5**) (Scheme 3). An attempt to prepare a monochloride compound by protonation of **4** with a sub-stoichiometric amount of HCl failed. Similarly, protonation of **4** with *p*-toluenesulfonic acid (HOTs) afforded the ditosylate compound [Ir(dtbpy)(CH_2CMe_2Ph)(OTs)$_2$] (**6**). In the ^{1}H NMR spectrum of **5**, the methylene protons of the neophyl ligands appear as two doublets at $\delta = 2.24$ and 2.58 ppm ($J = 11.1$ Hz), which are similar to those seen for **4**. The corresponding resonances for **6** are observed at more downfield positions ($\delta = 3.36$ and 3.50 ppm). As in the case of Pd–CH_2CMe_2Ph complexes,[29] treatment of **5** with bases resulted in orthometalation of the neophyl ligand. The cyclometalated compound [{Ir(dtbpy)($CH_2CMe_2C_6H_4$)}$_2$(μ-Cl)$_2$] (**7**) was most conveniently prepared by treatment of **5** with Li[BEt_3H]. The FAB mass spectrum of **7** shows the molecular ion at $m/z = 1256$, attributable to $[M^+ + 1]$, confirming the dinuclear nature of the compound.

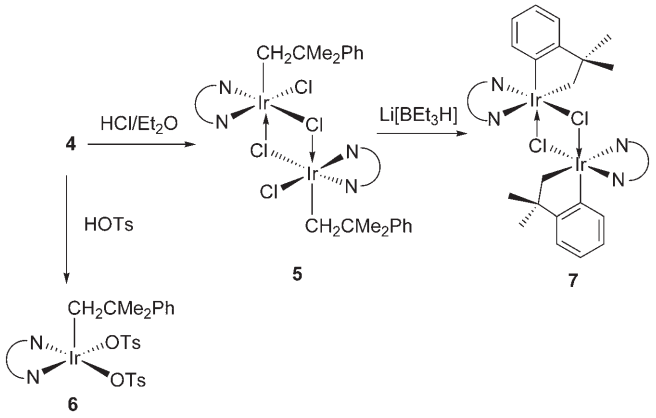

Scheme 3. Protonation of **4**.

The structure of **5** is shown in Figure 4; selected bond lengths and angles are listed in Table 5. The geometry about each Ir is pseudooctahedral with the neophyl ligand opposite to the μ-chloro ligand. The Ir–N distances (av. 2.018(4) Å) are similar to those in **4**. The Ir–C distance

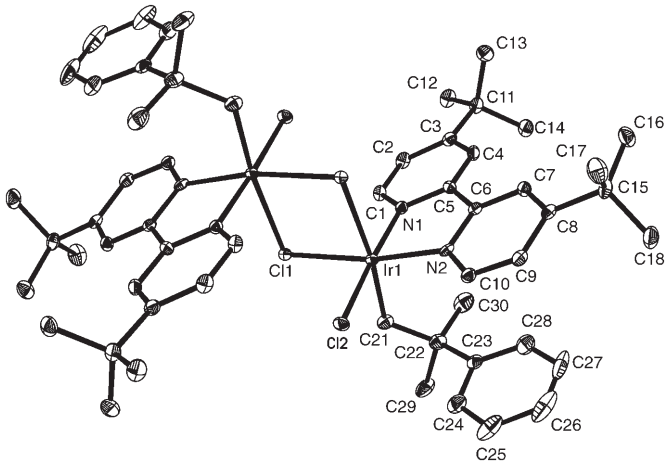

Figure 4. Molecular structure of [{Ir(dtbpy)(CH_2CMe_2Ph)Cl}$_2$(μ-Cl)$_2$] (**5**). Hydrogen atoms are omitted for clarity. The ellipsoids are drawn at a 40% probability level.

Table 5. Selected bond lengths [Å] and angles [°] for [{Ir(dtbpy)-(CH_2CMe_2Ph)Cl}$_2$(μ-Cl)$_2$] (**5**).

Ir1–N2	2.007(4)	Ir1–N1	2.029(4)
Ir1–C21	2.132(5)	Ir1–Cl2	2.383(1)
Ir1–Cl1	2.385(1)	Ir1–Cl1A	2.607(1)
N2-Ir1-N1	80.1(2)	N2-Ir1-C21	100.8(2)
N1-Ir1-C21	91.0(2)	N2-Ir1-Cl2	95.1(1)
N1-Ir1-Cl2	175.2(1)	C21-Ir1-Cl2	90.7(2)
N2-Ir1-Cl1	169.9(1)	N1-Ir1-Cl1	94.5(1)
C21-Ir1-Cl1	87.8(1)	Cl2-Ir1-Cl1	90.1(5)
N2-Ir1-Cl1 A	87.0(1)	N1-Ir1-Cl1A	89.2(1)
C21-Ir1-Cl1A	172.1(1)	Cl2-Ir1-Cl1A	89.7(4)
Cl1-Ir1-Cl1A	84.3(4)		

(2.132(5) Å) of the neophyl ligand in **5** is longer than the Ir–C(alkyl) distance in **4**. The two Ir–Cl(bridging) distances are not symmetric. The Ir–Cl(bridging, *trans* to C) distance (2.607(1) Å) is distinctly longer than the Ir–Cl(bridging, *trans* to N) distance (2.385(1) Å), which is similar to the Ir–Cl(terminal) distance (2.383(1) Å).

Oxidation of 4: The cyclic voltammogram of **4** in CH_2Cl_2 shows a reversible couple at 0.02 V versus $Cp_2Fe^{+/0}$ (ferrocenium/ferrocene) attributable to the Ir^{IV}–Ir^{III} couple, although the contribution of ligand-centered oxidation cannot be ignored. No oxidation couple was observed for the silyl alkyl compound **2**. By comparison, the Ir^{IV}–Ir^{III} couples for [Ir(mes)$_3$] [15b] and *fac*-[Ir(ppy)$_3$] (ppy = 2-(2-pyridyl)phenyl)[30] were found at 0.48 and 0.31 V versus $Cp_2Fe^{+/0}$, respectively, whereas that for [IrCp*Me$_2$(PPh$_3$)] appears at 0.41 V versus the saturated calomel electrode.[14b] The Ir^{IV}–Ir^{III} couple for the tetrakis-mesityl compound [Ir(mes)$_4$] was found at a considerably lower potential (−0.44 V versus $Cp_2Fe^{+/0}$).[16b]

The observation of a relatively low Ir^{IV}–Ir^{III} potential for **4** suggests that the Ir^{IV} state should be easily accessible. The oxidation of **4** with AgOTf (OTf^- = triflate) in CH_2Cl_2 has been monitored by using optical spectroscopy (Figure 5).

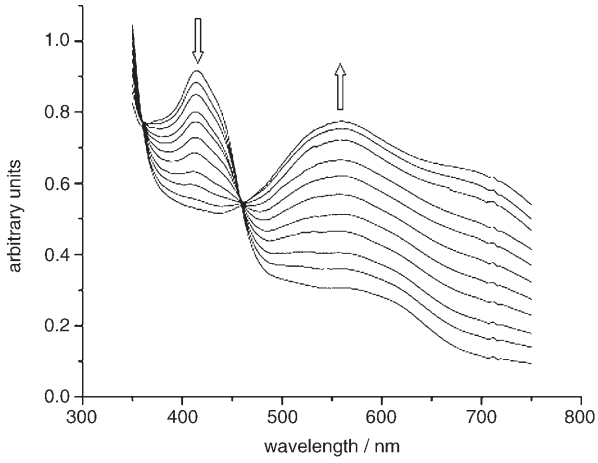

Figure 5. Optical spectral change for the oxidation of **4** with Ag(OTf) in CH_2Cl_2 (time interval = 2 min).

Upon addition of about one equivalent of AgOTf, the absorption at $\lambda = 420$ nm of **4** diminished and a broad absorption peak centered at $\lambda = 559$ nm appeared. The observation of well-defined isosbestic points at around $\lambda = 364$ and 463 nm indicates that no intermediate(s) accumulated during the oxidation of **4**. Upon addition of excess hexane to the reaction mixture, a purple-green solid, presumably [**4**(OTf)], was isolated. We have not been able to obtain an analytically pure sample of [**4**(OTf)]. In the absence of Ag^+, solutions containing [**4**(OTf)] are unstable and gradually decompose to **4**. The X-band electron paramagnetic resonance (EPR) spectrum of $\mathbf{4}^+$ in CH_2Cl_2 glass at 4 K displays an anisotropic signal with $g_\parallel = 2.430$ and $g_\perp = 2.110$, suggestive of an Ir^{IV} complex. No superhyperfine coupling with the ^{14}N nuclei was observed. By comparison, the EPR signal for [Ir^{IV}(mes)$_4$] was observed at $g_\parallel = 2.487$ and $g_\perp = 2.005$,[16b] whereas the g values for electrogenerated [IrCp*Me$_2$(PPh$_3$)]$^+$ are 2.387, 2.315, and 1.846.[14b]

Reaction of 4 with tetracyanoethylene: Although **4** is inert towards alkenes such as C_2H_4 and styrene, it was found to react with electron-deficient alkenes such as tetracyanœthylene (TCNE) and diethyl maleate. Treatment of **4** with TCNE in refluxing toluene gave a bluish-green mixture. Use of column chromatography led to the isolation of a blue complex **8** (18%), unreacted **4** (31%), and an uncharacterized purple species that was retained on the silica column (Scheme 4). Complex **8** was identified as the $C_2(CN)_3$-substit-

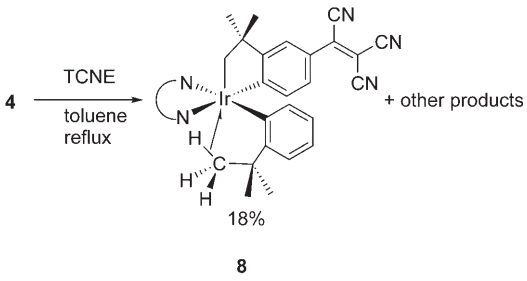

8

Scheme 4. Electrophilic substitution of **4** with TCNE.

uted iridacycle [Ir(dtbpy)($CH_2CMe_2C_6H_3$\{4-$C_2(CN)_3$\})(2-$C_6H_4CMe_3$)] by means of X-ray crystallography. The presence of the $C_2(CN)_3$ substituent in **8** was evidenced by using IR spectroscopy ($\tilde{\nu}$(CN) = 2214 and 2262 cm^{-1} cf. 2235 and 2276 cm^{-1} for free TCNE). Apparently, the formation of **8** involves electrophilic substitution of the iridacycle with TCNE and elimination of HCN. Activation of C–H bonds of σ-aryl ligands by electron-deficient alkenes such as TCNE is well documented.[31,32] Previously, insertion of TCNE into the C–H bonds of Pt^{II}-bound σ-furyl and -thienyl ligands has been reported by Onitsuka et al.[30]

Complex **8** has been unambiguously characterized by using X-ray crystallography (Figure 6); selected bond lengths and angles are given in Table 6. The geometry of **8** is similar to that of **4**, except that the methylene group instead

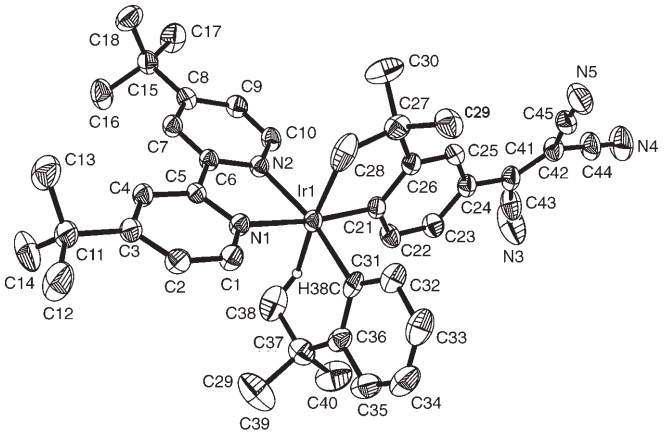

Figure 6. Molecular structure of [Ir(dtbpy)($CH_2CMe_2C_6H_3$\{4-$C_2(CN)_3$\})-(2-$C_6H_4CMe_3$)] (**8**). Hydrogen atoms other than the agostic hydrogen H38C are omitted for clarity. The ellipsoids are drawn at a 40% probability level.

Table 6. Selected bond lengths [Å] and angles [°] for [Ir(dtbpy)($CH_2CMe_2C_6H_3$\{4-$C_2(CN)_3$\})(2-$C_6H_4CMe_3$)] (**8**).

Ir1–C21	1.979(5)	Ir1–C31	2.051(5)
Ir1–C28	2.106(8)	Ir1–N2	2.123(4)
Ir1–N1	2.133(4)	Ir1–C38	2.556(8)
C21-Ir1-C31	90.8(2)	C21-Ir1-C28	82.9(2)
C31-Ir1-C28	99.2(3)	C21-Ir1-N2	99.3(2)
C31-Ir1-N2	168.7(2)	C28-Ir1-N2	87.0(2)
C21-Ir1-N1	172.7(2)	C31-Ir1-N1	94.4(2)
C28-Ir1-N1	76.0(2)	C21-Ir1-C38	101.8(2)
C31-Ir1-C38	77.7(2)	C28-Ir1-C38	174.3(3)
N2-Ir1-C38	95.2(2)	N1-Ir1-C38	84.3(2)

of the phenyl ring of the iridacycle is in the apical position. The Ir–C(alkyl) and Ir–C(aryl) distances (2.106(8) and 1.979(5) Å, respectively) in the iridacycle are comparable to those in **4**. As in the case of **4**, a δ agostic interaction was found for the 2-*tert*-butyphenyl ligand in **8**, with Ir···H-(agostic) and Ir–C(agostic) distances of 1.785(10) and 2.556(8) Å, respectively. The electrophilic substitution with TCNE occurred at the phenyl ring of the iridacycle instead of that of the 2-*tert*-butylphenyl ligand, possibly because the former is more electron-rich. In accordance with previous reports on electrophilic substitution of σ-aryl ligands,[33] the electrophilic attack on **4** occurred selectively *para* to the Ir–C(aryl) bond.

Iridafuran compound: Treatment of **4** with diethyl maleate in refluxing toluene resulted in elimination of *tert*-butylbenzene and the formation of the iridafuran compound [Ir(dtbpy)($CH_2CMe_2C_6H_4$)\{$\kappa^2(C,O)$-$C(CO_2Et)CH(CO_2Et)$\}] (**9**) (Scheme 5). Iridafuran compounds supported by phosphine[34–36] and tris(pyrazolyl)borate[37] co-ligands are well known. Recently, Dirnberger and Werner synthesized a related iridafuran compound [IrCl\{$\kappa^2(C,O)$-$C(CO_2Me)$=CH-(COMe)=O\}$H(P i Pr_3)_2$] by photochemical rearrangement and intramolecular C–H activation of the Ir^I dimethyl maleate complex *trans*-[IrCl\{η^2-(*E*)-$CHCO_2Me$=$CHCO_2Me$\}-($P i Pr_3)_2$]. Therefore, it seems that the iridafuran **9** was formed by oxidative addition of diethyl maleate to **4** and reductive elimination of *tert*-butylbenzene as shown in Scheme 6. The ^{13}C NMR spectrum of **9** displays resonances

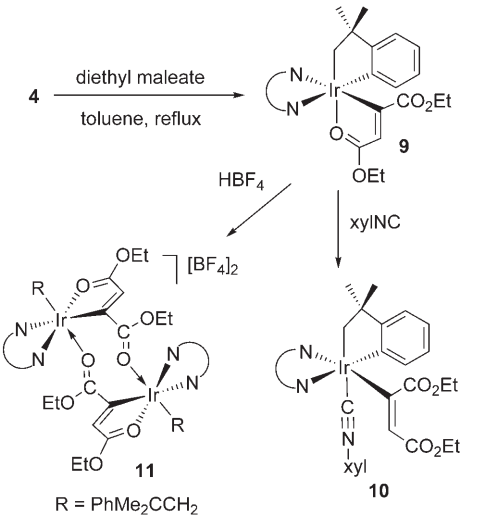

Scheme 5. Synthesis and reactivity of **9**.

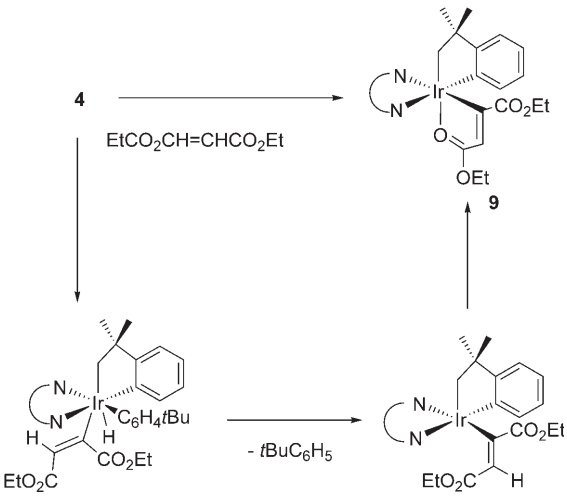

Scheme 6. Possible mechanism for the formation of **9**.

at $\delta = 195.7$, 179.9, and 183.3 ppm attributable to the iridafuran ring carbons C_α, C_β, and C_γ, respectively. The observed ^{13}C chemical shift for C_α of $\delta = 195.7$ ppm, which is similar to that for [Ir\{$\kappa^2(C,O)$-$C(CH_3)CHC(CH_3)(O)$\}$H(PEt_3)_3$]$^+$ ($\delta = 214.2$ ppm)[34] but further downfield than that for [IrCl\{$\kappa^2(C,O)$-$C(CO_2Me)$=CHC(COMe)=O\}$H(P i Pr_3)_2$] ($\delta =$ 178.9 ppm),[36] is indicative of carbenoid character.

Figure 7 shows a perspective view of **9**; selected bond lengths and angles are listed in Table 7. The geometry about the Ir is pseudooctahedral, with the methylene group of the iridacycle opposite to the oxygen atom of the iridafuran

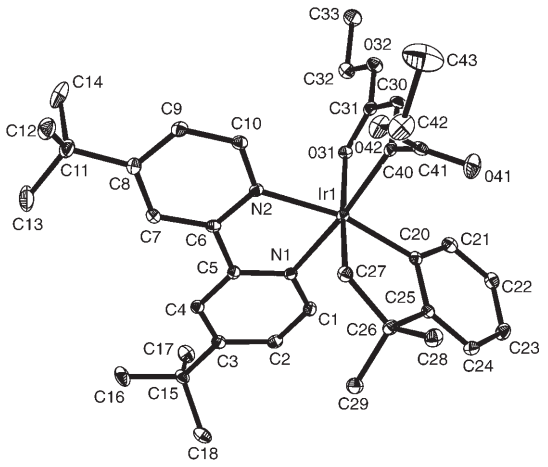

Figure 7. Molecular structure of [Ir(dtbpy)($CH_2CMe_2C_6H_4$){κ^2(*C*,*O*)-C(CO_2Et)CH(CO_2Et)}] (**9**). The ellipsoids are drawn at a 40% probability level.

Table 7. Selected bond lengths [Å] and angles [°] for [Ir(dtbpy)($CH_2CMe_2C_6H_4$){κ^2(*C*,*O*)-C(CO_2Et)CH(CO_2Et)}] (**9**).

Ir1–C40	1.993(3)	Ir1–C20	2.010(3)
Ir1–C27	2.057(3)	Ir1–N1	2.094(2)
Ir1–N2	2.110(2)	Ir1–O31	2.250(2)
C40–C30	1.351(4)	C30–C31	1.446(4)
C31–O31	1.237(4)		
C40-Ir1-C20	91.1(1)	C40-Ir1-C27	97.9(1)
C20-Ir1-C27	82.6(1)	C40-Ir1-N1	172.2(1)
C20-Ir1-N1	92.6(1)	C27-Ir1-N1	89.4(1)
C40-Ir1-N2	100.4(1)	C20-Ir1-N2	166.6(1)
C27-Ir1-N2	89.0(1)	N1-Ir1-N2	76.8(9)
C40-Ir1-O31	77.3(1)	C20-Ir1-O31	96.9(1)
C27-Ir1-O31	175.1(1)	N1-Ir1-O31	95.5(8)
N2-Ir1-O31	92.3(8)		

ring. The Ir–C(alkyl) and Ir–C(aryl) distances (2.057(3) and 2.010(3) Å, respectively) and the C-Ir-C′ angle (82.6(1)°) of the iridacycle are similar to those in **4**. In the iridafuran ring, the Ir–C_α (1.993(3) Å) and Ir–O_δ (2.250 Å) distances and the C_α-Ir-O_δ angle (77.3(1)°) are similar to those in [Ir{κ^2(*C*,*O*)-C(CH_3)CHC(CH_3)(O)}H(PEt_3)$_3$]$^+$ (2.029(6) and 2.206(4) Å and 77.0(2)°, respectively).[34] The C_γ–O_δ distance of 1.237(4) Å is intermediate between those for normal C–O single and double bonds. As previously suggested by Bleek and co-workers,[34] the overall bonding picture of the iridafuran ring in **9** can be represented by two resonance forms **A** and **B** (Scheme 7). Resonance structure **A** is supported by the short Ir–C_α distance (1.993(3) Å) and the downfield "carbenelike" chemical shift of C_α, whereas the relatively short C_γ–O_δ bond length is consistent with structure **B**.

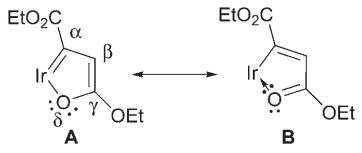

Scheme 7. Resonance structures of the iridafuran ring in **9**.

The Ir←O dative bond in the iridafuran ring in **9** is relatively weak and can be cleaved by strongly σ-donating, π-acceptor ligands. For example, treatment of **9** with 2,6-dimethylphenyl isocyanide (xylNC) afforded the vinyl compound [Ir(dtbpy)($CH_2CMe_2C_6H_4$){C(CO_2Et)CH(CO_2Et)}(xylNC)] (**10**). The IR spectrum of **9** shows the $\tilde{\nu}$(C≡N) band at 2099 cm^{-1}, indicating that the isocyanide binds to the Ir without insertion into an Ir–C bond.

Compound **10** has been characterized by using X-ray crystallography. The asymmetric unit consists of two independent molecules. The structure of one of these molecules is shown in Figure 8; selected bond lengths and angles are

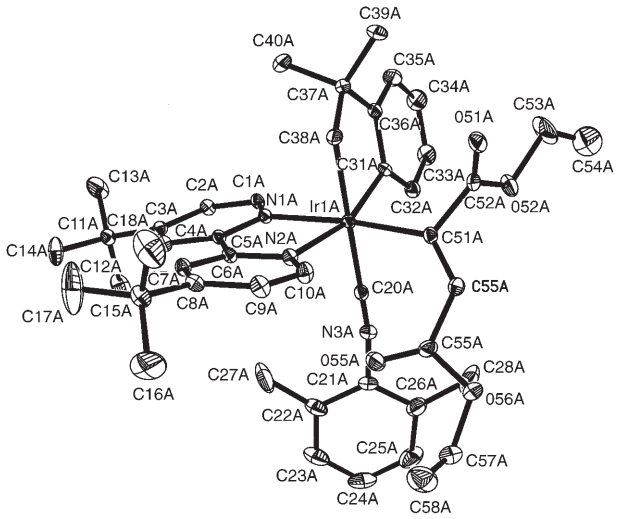

Figure 8. Molecular structure of one of the two independent molecules in the asymmetric unit of [Ir(dtbpy)($CH_2CMe_2C_6H_4$){C(CO_2Et)CH(CO_2Et)}(xylNC)] (**10**). The ellipsoids are drawn at a 40% probability level.

listed in Table 8. The structure of **10** is similar to that of **9**, except that the oxygen atom in the iridafuran ring in **9** is replaced by the isocyanide ligand. The Ir–C(alkyl) distance in the iridacycle (av. 2.108(4) Å) is slightly longer than that in **9** (2.010(3) Å), but the Ir–C(aryl) distance (av. 2.036(4) Å) is similar to that in **9** (2.057(3) Å). The Ir–C_α distance in **10** (av. 2.048 Å) is slightly longer than that in **9** (1.993(3) Å), whereas the C–O distance in **10** (av. 1.199 Å) is slightly shorter than that in **9** (1.237(4) Å), suggesting that cleavage of the iridafuran ring decreases the π-conjugation across the Ir–C_α–C_β–C_γ–O_δ unit.

Treatment of **9** with HBF_4 led to cleavage of the Ir($CH_2CMe_2C_6H_4$) metallacycle and the formation of the dinuclear neophyl compound [(Ir(dtbpy)(CH_2CMe_2Ph){κ^2(*C*,*O*)-C(CO_2Et)CH(CO_2Et)}$_2$][BF_4]$_2$ (**11**). It may be noted that the protonation occurred selectively at the Ir($CH_2CMe_2C_6H_4$) metallacycle rather than at the iridafuran ring. Upon cleavage of the Ir($CH_2CMe_2C_6H_4$) metallacycle, the resonances of the methylene protons shift downfield

Table 8. Selected bond lengths [Å] and angles [°] for [[Ir(dtbpy)-($CH_2CMe_2C_6H_4$){C(CO_2Et)CH(CO_2Et)}(xylNC)] (**10**).

Ir1A–C20A	1.962(4)	Ir1A–C51A	2.046(4)
Ir1A–C31A	2.057(4)	Ir1A–C38A	2.106(4)
Ir1A–N1A	2.112(3)	Ir1A–N2A	2.141(3)
Ir1B–C20B	1.967(4)	Ir1B–C31B	2.014(4)
Ir1B–C51B	2.050(4)	Ir1B–C38B	2.110(4)
Ir1B–N2B	2.112(3)	Ir1B–N1B	2.124(3)
C20A-Ir1A-C51A	88.21(15)	C20A-Ir1A-C31A	94.51(16)
C51A-Ir1A-C31A	92.17(15)	C20A-Ir1A-C38A	175.31(17)
C51A-Ir1A-C38A	93.95(15)	C31A-Ir1A-C38A	81.27(17)
C20A-Ir1A-N1A	88.73(13)	C51A-Ir1A-N1A	173.71(14)
C31A-Ir1A-N1A	93.55(13)	C38A-Ir1A-N1A	89.51(13)
C20A-Ir1A-N2A	98.63(14)	C51A-Ir1A-N2A	98.79(14)
C31A-Ir1A-N2A	163.11(14)	C38A-Ir1A-N2A	85.16(14)
N1A-Ir1A-N2A	76.26(11)	C20B-Ir1B-C31B	94.55(15)
C20B-Ir1B-C51B	91.24(15)	C31B-Ir1B-C51B	89.52(14)
C20B-Ir1B-C38B	173.38(15)	C31B-Ir1B-C38B	81.16(15)
C51B-Ir1B-C38B	93.75(15)	C20B-Ir1B-N2B	87.14(12)
C51B-Ir1B-N2B	174.98(13)	C38B-Ir1B–N2B	88.24(13)
C20B-Ir1B-N1B	96.02(13)	C31B-Ir1B-N1B	166.07(13)

from $\delta = 1.03$ and 2.64 (d, $J = 10.5$ Hz) for **9** to $\delta = 2.49$ and 3.15 ppm (d, $J = 18$ Hz) for **11**, which are comparable to those for the neophyl compound **5** ($\delta = 2.24$ and 2.58 ppm).

Figure 9 shows a perspective view of the dication [Ir(dtbpy)(CH_2CMe_2Ph){κ^2(*C*,*O*)-C(CO_2Et)CH(CO_2Et)}]$_2^{2+}$ in **11**; selected bond lengths and angles are listed in Table 9. The structure of **11** consists of two [Ir(dtbpy)-

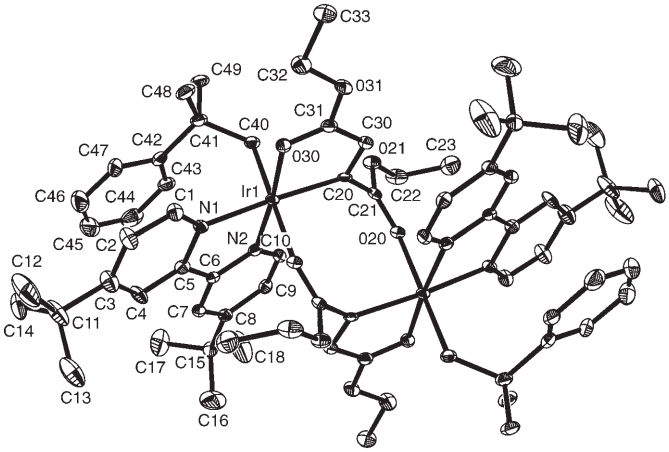

Figure 9. Structure of the dication [Ir(dtbpy)(CH_2CMe_2Ph){κ^2(*C*,*O*)-C(CO_2Et)CH(CO_2Et)}]$_2^{2+}$ in **11**. The ellipsoids are drawn at a 40% probability level.

(CH_2CMe_2Ph){κ^2(*C*,*O*)-C(CO_2Et)CH(CO_2Et)}]$^+$ fragments that are linked together by the CO_2Et side chains of the iridafuran rings. In each [Ir(dtbpy)(CH_2CMe_2Ph){κ^2(*C*,*O*)-C(CO_2Et)CH(CO_2Et)}]$^+$ fragment, the geometry about the Ir is pseudooctahedral with the iridafuran ring opposite to the dtbpy ligand. The whole molecule is related by an inversion center located at the center of the eight-membered $C_4O_2Ir_2$ ring, which has a pseudochair conformation (Figure 10). The

Table 9. Selected bond lengths [Å] and angles [°] for [(Ir(dtbpy)-(CH_2CMe_2Ph){κ^2(*C*,*O*)-C(CO_2Et)CH(CO_2Et)})$_2$][BF_4]$_2$ (**11**).

Ir1–C40	2.075(4)	Ir1–C20	2.023(5)
Ir1–N1	2.066(4)	Ir1–N2	2.022(4)
Ir1–O30	2.083(4)	Ir1–O20A	2.249(3)
C20–C30	1.360(7)	C30–C31	1.446(8)
C31–O20	1.253(6)		
C40-Ir1-C20	85.8(2)	C40-Ir1-N1	102.3(2)
C20-Ir1-N1	170.4(2)	C40-Ir1-N2	89.3(2)
C20-Ir1-N2	106.9(2)	N1-Ir1-N2	78.8(2)
C40-Ir1-O30	91.1(2)	C20-Ir1-O30	78.9(2)
N1-Ir1-O30	95.5(2)	N2-Ir1-O30	174.2(2)
N2-Ir1-O20A	93.9(2)	C20-Ir1-O20A	94.7(2)
N1-Ir1-O20A	76.9(2)	C40-Ir1-O20A	176.5(2)
O30-Ir1-O20A	85.6(1)		

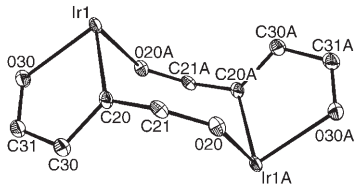

Figure 10. View of the eight-membered $C_4O_2Ir_2$ ring in **11** showing the pseudochair conformation. The ellipsoids are drawn at a 40% probability level.

Ir–C_α distance (2.023(5) Å) and O_δ-Ir-C_α angle (78.9(2)°) in the iridafuran ring are similar to those in **9**. The Ir–O_δ bond *trans* to nitrogen (2.083(4) Å) is distinctly shorter than the Ir–O bond *trans* to the neophyl ligand (2.249(3) Å). As in **9**, the observed downfield chemical shift for C_α ($\delta =$ 195.7 ppm) and the relatively short Ir–C_α (2.023(5) Å) and C_γ–O_δ distances (1.253(6) Å) suggest that the overall bonding picture of the iridafuran ring in **11** can be represented by two resonance forms **A** and **B** (Scheme 7).

Conclusion

In summary, we have synthesized dtbpy-supported Ir^{III} alkyl compounds by transmetalation of [$IrCl_3$(dmf)(dtbpy)] with Me_3SiCH_2MgCl and $PhMe_2CCH_2MgCl$. The alkylation with Me_3SiCH_2MgCl resulted in C–Si cleavage and formation of the Ir silyl dialkyl complex **2**, whereas that with $PhMe_2CCH_2MgCl$ afforded the iridacycle **4**. Complex **2** was found to react with phenylacetylene to give a dimeric silyl dialkynyl compound. The iridacycle **4** is electron-rich and can be reversibly oxidized with Ag^I to give an Ir^{IV} alkyl complex, which has been characterized by means of EPR spectroscopy. Although **4** is inert towards alkanes and alkenes under normal conditions, reactions of **4** with TCNE and diethyl maleate led to electrophilic substitution of the iridacycle and to formation of an iridafuran compound, respectively. The above results illustrate some interesting organometallic reactivity exhibited by the Ir^{III}(dtbpy) core, which has yet to be fully explored. In the future, efforts will be direct-

ed towards the synthesis of cationic, unsaturated Ir(dtpby) alkyl complexes that may find application in the activation of C–H bonds of hydrocarbons.

Experimental Section

General: All manipulations were carried out under nitrogen by using standard Schlenk techniques. Solvents were purified, distilled, and degassed prior to use. NMR spectra were recorded on a Varian Mercury 300 spectrometer operating at 300, 121.5, and 282.4 MHz for ^{1}H, ^{31}P, and ^{19}F, respectively. Chemical shifts (δ, ppm) are reported with reference to $SiMe_4$ (^{1}H and ^{13}C), $P(OCH_3)_3$ (^{31}P), and $C_6H_5CF_3$ (^{19}F). Infrared spectra were recorded on a Perkin–Elmer 16 PC FTIR spectrophotometer, mass spectra on a Finnigan TSQ 7000 spectrometer. Cyclic voltammetry was performed with a Princeton Applied Research (PAR) model 273 A potentiostat. The working and reference electrodes consisted of glassy carbon and $Ag/AgNO_3$ (0.1 M in acetonitrile), respectively. Reduction potentials were determined in CH_2Cl_2 with 0.1 M $[n Bu_4N][PF_6]$ as supporting electrolyte at a scan rate of 100 $mV s^{-1}$, and are reported with reference to the ferrocenium/ferrocene couple. X-band EPR spectra were recorded on a Bruker EMX EPR spectrometer equipped with a variable-temperature helium flow cryostat system (Oxford Instruments). Elemental analyses were performed by Medac Ltd., Surrey, UK. Hydrogen atom labeling schemes for the dtbpy ligand and the iridacyclic compound are shown below.

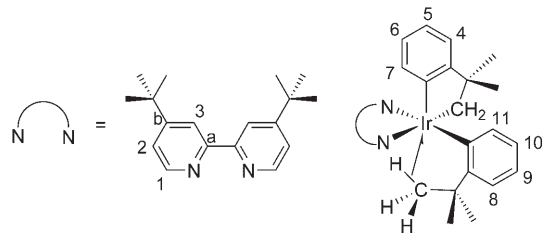

Preparation of [$IrCl_3$(dmf)(dtbpy)] (1): 4,4′-Di-*tert*-butyldipyridyl (dtbpy) (120 mg, 0.448 mmol) was added to a solution of $IrCl_3 \cdot x H_2O$ (150 mg, 0.445 mmol) in *N*,*N*-dimethylformamide (dmf) (2 mL) and the mixture was heated under reflux for 3 h. Et_2O (20 mL) was added to the cooled solution and the orange precipitate formed was collected and washed with Et_2O. Yield: 210 mg (74%); ^{1}H NMR (300 MHz, $CDCl_3$): $\delta = 1.44$ (s, 9H; *t*Bu), 1.46 (s, 9H; *t*Bu), 3.21 (s, 3H; CH_3), 3.25 (s, 3H; CH_3), 7.49 (dd, $J = 6.6$, 1.8 Hz, 1H; H^2), 7.60 (dd, $J = 6.6$, 1.8 Hz, 1H; H^2), 7.92 (d, $J = 1.8$ Hz, 1H; H^3), 7.98 (d, $J = 1.8$ Hz, 1H; H^3), 8.30 (s, 1H; CHO), 8.87 (d, $J = 6$ Hz, 1H; H^1), 9.70 ppm (d, $J = 4.2$ Hz, 1H; H^1); MS (FAB): *m*/*z*: 567.9 [$M^+ + 1 - dmf$]; elemental analysis calcd (%) for $C_{21}H_{31}N_3OCl_3Ir \cdot 2H_2O$ (675.14): C 37.31, H 5.22, N 6.22; found: C 37.60, H 4.99, N 6.22.

Preparation of [$Ir(CH_2SiMe_3)$(dtbpy)(Me)($SiMe_3$)] (2): Me_3SiCH_2MgCl (0.78 mL of a 0.8 M solution in THF, 0.625 mmol) was added to a suspension of **1** (100 mg, 0.156 mmol) in THF (25 mL) at −78 °C. The mixture was allowed to warm to room temperature and stirred overnight. The volatiles were then removed in vacuo and the residue was extracted with hexane. The extracts were concentrated and cooled to −40 °C to give reddish-brown crystals suitable for X-ray diffraction analysis. Yield: 63 mg (63%); ^{1}H NMR (300 MHz, C_6D_6): $\delta = 0.12$ (s, 9H; $CH_2Si\mathit{Me}_3$), 0.33 (s, 9H; $SiMe_3$), 1.01 (s, 18H; *t*Bu), 2.13 (d, $J = 11.7$ Hz, 1H; CH_2SiMe_3), 2.34 (s, 3H; CH_3), 2.47 (d, $J = 11.7$ Hz, 1H; CH_2SiMe_3), 6.63 (s, 1H; H^2), 6.80 (s, 1H; H^2), 7.59 (s, 1H; H^3), 7.63 (s, 1H; H^3), 9.43 (d, $J = 6.0$ Hz, 1H; H^1), 9.46 ppm (d, $J = 6.0$ Hz, 1H; H^1); $^{13}C\{^{1}H\}$ NMR (C_6D_6): $\delta = 125.3$ (C^1), 124.6 (C^1), 124.3 (C^2), 123.8 (C^a), 123.4 (C^b), 123.2 (C^2), 120.8 (C^a), 120.2 (C^b), 119.3 (C^3), 118.4 (C^3), 30.9 ($C\mathit{Me}_3$), 30.2 ($C\mathit{Me}_3$), 23.2 ($C\mathit{Me}_3$), 22.1 (Me), 16.2 (CH_2SiMe_3), 12.2 ($C\mathit{Me}_3$), 0.89 ($Si\mathit{Me}_3$), −5.11 ppm ($CH_2Si\mathit{Me}_3$); MS (FAB): *m*/*z*: 563.0 [$M^+ - SiMe_3$]; elemental analysis calcd (%) for $C_{26}H_{47}N_2Si_2Ir$ (636.29): C 49.10, H 7.45, N 4.40; found: C 49.21, H 7.64, N 4.26.

Preparation of [Ir(*t*BuNC)(CH_2SiMe_3)(dtbpy)(Me)($SiMe_3$)] ([2-(*t*BuNC)]): *tert*-Butyl isocyanide (7 mg, 0.084 mmol) was added to a solution of **2** (50 mg, 0.079 mmol) in CH_2Cl_2 (25 mL) and the mixture was stirred at room temperature overnight. The volatiles were then removed in vacuo and the residue was extracted with Et_2O/hexane. The extracts were concentrated and cooled to 0 °C to give a brown powder. Yield: 47 mg (83%); ^{1}H NMR (300 MHz, C_6D_6): $\delta = -0.03$ (s, 9H; $CH_2Si\mathit{Me}_3$), 0.41 (s, 2H; $C\mathit{H}_2SiMe_3$), 0.63 (s, 9H; $SiMe_3$), 0.88 (s, 9H; *t*Bu), 0.96 (s, 9H; *t*Bu), 1.06 (s, 9H; *t*BuNC), 1.40 (s, 3H; CH_3), 6.64 (dd, $J = 6.3$, 2.1 Hz, 1H; H^2), 6.72 (dd, $J = 6$, 2.1 Hz, 1H; H^2), 7.71 (d, $J = 1.8$ Hz, 1H; H^3), 7.80 (d, $J = 1.8$ Hz, 1H; H^3), 9.16 (d, $J = 6$ Hz, 1H; H^1), 9.21 ppm (d, $J = 6$ Hz, 1H; H^1); IR (KBr): $\tilde{\nu} = 2096\ cm^{-1}$ (C≡N); MS (FAB): *m*/*z*: 646.3 [$M^+ - SiMe_3$]; elemental analysis calcd (%) for $C_{31}H_{56}N_3Si_2Ir \cdot 1.5 CH_2Cl_2 \cdot Et_2O$ (919.37): C 47.62, H 7.55, N 4.56; found: C 47.13, H 8.08, N 4.25.

Preparation of [{Ir(C≡CPh)(dtbpy)($SiMe_3$)}$_2$(μ-C≡CPh)$_2$] (3): Phenylacetylene (16 mg, 0.157 mmol) was added to a solution of **2** (50 mg, 0.079 mmol) in benzene (10 mL). The mixture was stirred at room temperature for 10 min and then left to stand overnight. Red crystals were deposited, which were collected and washed with hexane. Yield: 72 mg (31%); satisfactory NMR data for **3** were not obtained; IR (KBr): $\tilde{\nu} =$ 2050, 2097 cm^{-1} (C≡C); MS (FAB): *m*/*z*: 664.2 [$1/2\,M^+ + 1 - SiMe_3$], 1401.5 [$M^+ + 2 - SiMe_3$]; elemental analysis calcd (%) for $C_{74}H_{86}N_4Si_2Ir_2 \cdot H_2O$ (1490.58): C 59.65, H 5.95, N 3.76; found: C 59.55, H 5.87, N 3.69.

Preparation of [Ir(dtbpy)($CH_2CMe_2C_6H_4$)(2-$C_6H_4CMe_3$)] (4): $PhMe_2C$-CH_2MgCl (0.78 mL of a 0.8 M solution in THF, 0.625 mmol) was added to a suspension of **1** (100 mg, 0.156 mmol) in THF (25 mL) at −78 °C. The mixture was allowed to warm to room temperature and stirred overnight. The volatiles were then removed in vacuo and the residue was recrystallized from hexane at −10 °C to give dark yellowish-green crystals suitable for X-ray diffraction analysis. Yield: 98 mg (87%); ^{1}H NMR (300 MHz, $CDCl_3$): $\delta = 0.81$ (s, 9H; $C_6H_4C\mathit{Me}_3$), 0.91 (s, 6H; $C_6H_4C\mathit{Me}_2CH_2$), 1.41 (s, 9H; *t*Bu), 1.47 (s, 9H; *t*Bu), 2.74 (d, $J = 10.5$ Hz, 1H; $C_6H_4CMe_2C\mathit{H}_2$), 2.94 (d, $J = 10.5$ Hz, 1H; $C_6H_4CMe_2C\mathit{H}_2$), 5.54 (d, $J = 7.5$ Hz, 1H; H^8), 6.30 (dt, $J = 5.7$, 3.3 Hz, 1H; H^9), 6.59–6.61 (m, 2H; H^4 and H^5), 6.64–6.66 (m, 2H; H^{10} and H^{11}), 6.82 (dt, $J = 5.7$, 3.3 Hz, 1H; H^6), 7.01 (d, $J = 7.5$ Hz, 1H; H^7), 7.37 (d, $J = 1.8$ Hz, 1H; H^2), 7.39 (d, $J = 1.8$ Hz, 1H; H^2), 8.03 (d, $J = 1$ Hz, 1H; H^3), 8.09 (d, $J = 1$ Hz, 1H; H^3), 8.40 (d, $J = 5.7$ Hz, 1H; H^1), 9.14 ppm (d, $J = 5.7$ Hz, 1H; H^1); $^{13}C\{^{1}H\}$ NMR ($CDCl_3$): $\delta =$ 165.9 ($C_6H_4CMe_2CH_2$), 160.2 (C^a), 160.1 (C^b), 157.6 ($C_6H_4CMe_3$), 157.5 (C^a), 157.3 (C^b), 149.8 (C^1), 148.1 (C^1), 148.0 ($C_6H_4CMe_3$), 139.5 ($C_6H_4CMe_2CH_2$), 138.2 (C^5), 129.1 (C^8), 124.9 (C^7), 124.7 (C^2), 124.0 (C^4), 123.7 (C^2), 123.5 (C^{10}), 123.1 (C^9), 120.6 (C^{11}), 120.2 (C^6), 119.3 (C^3), 118.9 (C^3), 45.8 ($C\mathit{Me}_3$), 39.3 ($C\mathit{Me}_3$), 36.6 ($C_6H_4C\mathit{Me}_2CH_2$), 35.9 ($C_6H_4C\mathit{Me}_2CH_2$), 35.6 ($C_6H_4C\mathit{Me}_2CH_2$), 31.0 ($C\mathit{Me}_3$), 30.9 ($C\mathit{Me}_3$), 30.0 ($C_6H_4C\mathit{Me}_3$), 22.8 ($C_6H_4CMe_2C\mathit{H}_2$), 14.7 ppm ($C_6H_4CMe_3$); MS (FAB): *m*/*z*: 726.3 [$M^+ + 1$]; elemental analysis calcd (%) for $C_{38}H_{49}N_2Ir \cdot 0.5 C_6H_{14}$ (769.41): C 64.03, H 7.34, N 3.64; found: C 64.24, H 7.52, N 3.55.

Oxidation of 4 with Ag(OTf): Ag(OTf) (18 mg, 0.070 mmol, 1 equiv) was added to a solution of **4** (50 mg, 0.069 mmol) in CH_2Cl_2 (15 mL) and the mixture was stirred at room temperature for 1 h. The solvent was then removed and the residue was extracted with CH_2Cl_2. Addition of hexane to the extract afforded a purple solid, presumably having the composition [**4**(OTf)] (32 mg). We were unable to obtain an analytically pure sample of [**4**(OTf)]. An attempt to recrystallize [**4**(OTf)] from CH_2Cl_2/hexane led to recovery of **4**. UV/Vis (CH_2Cl_2): $\lambda_{max} =$ 559, 700 nm; EPR (4 K, CH_2Cl_2): $g_{\parallel} = 2.430$ and $g_{\perp} = 2.110$.

Preparation of [{Ir(dtbpy)(CH_2CMe_2Ph)Cl}$_2$(μ-Cl)$_2$] (5): HCl (0.09 mL of a 1.5 M solution in Et_2O, 0.065 mmol) was added to a solution of **4** (100 mg, 0.138 mmol) in hexane (10 mL) at 0 °C. The reaction mixture was stirred at room temperature for 2 h. A red precipitate was deposited, which was collected, washed with Et_2O, and recrystallized from CH_2Cl_2/hexane to give red crystals suitable for X-ray diffraction analysis. Yield: 75 mg (82%); ^{1}H NMR (300 MHz, $CDCl_3$): $\delta = 0.84$ (s, 6H; $CH_2C\mathit{Me}_2Ph$), 0.87 (s, 6H; $CH_2C\mathit{Me}_2Ph$), 1.42 (s, 18H; *t*Bu), 1.45 (s, 18H;

*t*Bu), 2.24 (d, $J=11.1$ Hz, 2H; CH_2CMe_2Ph), 2.58 (d, $J=11.1$ Hz, 2H; CH_2CMe_2Ph), 6.14 (d, $J=8.4$ Hz, 2H; CH_2CMe_2Ph), 6.21 (d, $J=8.4$ Hz, 4H; CH_2CMe_2Ph), 6.30 (t, $J=7.5$ Hz, 4H; CH_2CMe_2Ph), 6.73 (d, $J=5.6$ Hz, 2H; H^2), 6.83 (d, $J=7.8$ Hz, 2H; H^2), 7.37 (dd, $J=5.7$, 1.8 Hz, 2H; H^3), 7.49 (dd, $J=6.3$, 2.1 Hz, 2H; H^3), 9.76 (d, $J=6.3$ Hz, 2H; H^1), 10.27 ppm (d, $J=6.6$ Hz, 2H; H^1); MS (FAB): *m/z*: 1294 [M^++1−Cl]; elemental analysis calcd (%) for $C_{56}H_{74}N_4Cl_4Ir_2$ (1328.40): C 51.07, H 5.84, N 4.01; found: C 50.59, H 5.61, N 4.21.

Preparation of [Ir(dtbpy)(CH_2CMe_2Ph)($OTs)_2$] (6): HOTs (48 mg, 0.279 mmol) was added to a solution of **4** (100 mg, 0.138 mmol) in dichloromethane (10 mL) at 0 °C and the mixture was stirred at room temperature for 2 h. The volatiles were then removed in vacuo and the residue was washed with Et_2O. Recrystallization from CH_2Cl_2/hexane gave a yellow powder. Yield: 82 mg (63 %); ^{1}H NMR (300 MHz, $CDCl_3$): $\delta=$ 1.11 (s, 3H; CH_2CMe_2Ph), 1.18 (s, 3H; CH_2CMe_2Ph), 1.42 (s, 9H; *t*Bu), 1.43 (s, 9H; *t*Bu), 2.26 (s, 3H; OTs), 2.32 (s, 3H; OTs), 3.36 (d, $J=$ 10.8 Hz, 1H; CH_2CMe_2Ph), 3.50 (d, $J=10.8$ Hz, 1H; CH_2CMe_2Ph), 6.41 (d, $J=7.2$ Hz, 2H; CH_2CMe_2Ph), 6.57 (t, $J=7.5$ Hz, 2H; CH_2CMe_2Ph), 6.77 (t, $J=7.5$ Hz, 1H; CH_2CMe_2Ph), 6.92 (d, $J=8.1$ Hz, 2H; OTs), 7.04 (d, $J=7.8$ Hz, 2H; OTs), 7.28–7.37 (m, 6H; OTs and H^2), 7.86 (d, $J=$ 8.1 Hz, 2H; H^3), 8.50 (d, $J=6.0$ Hz, 1H; H^1), 8.73 ppm (d, $J=5.7$ Hz, 1H; H^1); MS (FAB): *m/z*: 936 [M^++1]; elemental analysis calcd (%) for $C_{42}H_{51}N_2O_6S_2Ir\cdot CH_2Cl_2$ (1020.24): C 50.58, H 5.23, N 2.74; found: C 50.50, H 5.43, N 2.65.

Preparation of [{Ir(dtbpy)($CH_2CMe_2C_6H_4$)}$_2$(μ-Cl)$_2$] (7): Li[BEt_3H] (0.048 mL of a 1.5 M solution in THF, 0.072 mmol) was added to a suspension of **5** (50 mg, 0.036 mmol) in THF (25 mL) at −78 °C and the mixture was stirred at this temperature for 1 h. It was then allowed to warm to room temperature and stirred overnight. The volatiles were subsequently removed in vacuo and the residue was extracted with hexane. Concentration of the extracts and cooling to −10 °C gave a greenish-brown powder. Yield: 38 mg (84 %); ^{1}H NMR (300 MHz, C_6D_6): $\delta=0.74$ (s, 9H; *t*Bu), 1.18 (s, 9H; *t*Bu), 1.34 (s, 3H; CH_2CMe_2Ph), 1.96 (s, 3H; CH_2CMe_2Ph), 1.98 (d, $J=13.2$ Hz, 1H; CH_2CMe_2Ph), 2.97 (d, $J=13.2$ Hz, 1H; CH_2CMe_2Ph), 5.76 (dd, $J=6.6$, 2.1 Hz, 1H; H^4), 7.01 (dt, $J=7.0$, 2.1 Hz, 1H; H^5), 7.12 (dt, $J=7.2$, 1.8 Hz, 1H; H^6), 7.35–7.38 (m, 3H; H^7 and H^2), 7.64 (d, $J=7.2$ Hz, 1H; H^3), 8.57 (d, $J=7.2$ Hz, 1H; H^3), 8.66 (d, $J=$ 6.3 Hz, 1H; H^1), 9.40 ppm (d, $J=6.0$ Hz, 1H; H^1); MS (FAB): *m/z*: 1256 [M^++1]; elemental analysis calcd (%) for $C_{28}H_{36}N_2ClIr\cdot C_6H_{14}$ (714.33): C 56.73, H 6.12, N 4.73; found: C 56.34, H 6.10, N 4.12.

Preparation of [Ir(dtbpy)($CH_2CMe_2C_6H_3${4-$C_2(CN)_3$})(2-$C_6H_4CMe_3$)] (8): Tetracyanoethylene (18 mg, 0.141 mmol) was added to a solution of **4** (100 mg, 0.138 mmol) in toluene (10 mL). The mixture was heated under reflux overnight and then concentrated to dryness. The residue was redissolved in CH_2Cl_2 and loaded onto a column of silica gel for column chromatography. Unreacted **4** was eluted with Et_2O. Yield: 31 mg (31 %). The product was eluted with CH_2Cl_2/acetone (9:1) as a blue band and was recrystallized from CH_2Cl_2/hexane to give blue crystals suitable for X-ray diffraction analysis. Yield: 20 mg (18 %); ^{1}H NMR (300 MHz, $CDCl_3$): $\delta=0.92$ (s, 9H; $C_6H_4CMe_3$), 1.42 (s, 9H; *t*Bu), 1.44 (s, 3H; $C_6H_3CMe_2CH_2$), 1.46 (s, 3H; $C_6H_3CMe_2CH_2$), 1.48 (s, 9H; *t*Bu), 2.75 (d, $J=11.4$ Hz, 1H; $C_6H_3CMe_2CH_2$), 2.93 (d, $J=11.7$ Hz, 1H; $C_6H_3CMe_2CH_2$), 5.54 (d, $J=7.5$ Hz, 1H; H^8), 6.27–6.35 (m, 1H; H^9), 6.71 (d, $J=7.5$ Hz, 2H; H^{10} and H^{11}), 6.98 (d, $J=8.4$ Hz, 1H; H^6), 7.10–7.18 (m, 1H; H^4), 7.47 (d, $J=7.8$ Hz, 1H; H^7), 7.80 (d, $J=2.4$ Hz, 1H; H^2), 8.05 (d, $J=5.7$ Hz, 1H; H^1), 8.08 (d, $J=1.8$ Hz, 2H; H^3), 8.15 (d, $J=$ 1.8 Hz, 1H; H^2), 9.02 ppm (d, $J=5.7$ Hz, 1H; H^1); IR (KBr): $\tilde{\nu}=2214$, 2262 cm^{-1} (C≡N); MS (FAB): *m/z*: 827.3 [M^++1]; elemental analysis calcd (%) for $C_{43}H_{48}N_5Ir\cdot 2CH_2Cl_2\cdot C_6H_{14}$ (1081.37): C 56.55, H 6.14, N 6.47; found: C 57.02, H 6.35, N 6.78.

Preparation of [Ir(dtbpy)($CH_2CMe_2C_6H_4$){κ^2(*C*,*O*)-C(CO_2Et)CH(CO_2Et)}] (9): Diethyl maleate (24 mg, 0.139 mmol) was added to a solution of **4** (100 mg, 0.138 mmol) in toluene (10 mL). The mixture was heated under reflux overnight, then concentrated to dryness, and the residue was subjected to column chromatography on silica gel. The product was eluted with hexane/CH_2Cl_2 (9:1) and recrystallized from CH_2Cl_2/hexane to give reddish-brown crystals suitable for X-ray diffraction analysis. Yield: 78 mg (74 %); ^{1}H NMR (300 MHz, $CDCl_3$): $\delta=0.60$ (s, 3H; $C_6H_4CMe_2CH_2$), 0.90 (t, $J=6.6$ Hz, 3H; $CO_2CH_2CH_3$), 1.03 (d, $J=$ 10.5 Hz, 1H; $C_6H_4CMe_2CH_2$), 1.11 (s, 3H; $C_6H_4CMe_2CH_2$), 1.16 (t, $J=$ 7.2 Hz, 3H; $CO_2CH_2CH_3$), 1.40 (s, 9H; *t*Bu), 1.43 (s, 9H; *t*Bu), 2.64 (d, $J=10.5$ Hz, 1H; $C_6H_4CMe_2CH_2$), 3.95–4.34 (m, 4H; $CO_2CH_2CH_3$), 6.70 (dd, $J=7.2$, 1.8 Hz, 1H; H^4), 6.75 (s, 1H; C=C*H*CO_2Et), 6.79 (dd, $J=7.2$, 1.8 Hz, 1H; H^7), 6.87 (dt, $J=6.0$, 1.2 Hz, 2H; H^5 and H^6), 7.17 (dd, $J=$ 5.7, 1.8 Hz, 1H; H^2), 7.38 (dd, $J=5.7$, 1.8 Hz, 1H; H^2), 8.00 (d, $J=1.8$ Hz, 2H; H^3), 8.15 (d, $J=5.7$ Hz, 1H; H^1), 8.91 ppm (d, $J=6.0$ Hz, 1H; H^1); ^{13}C{^{1}H} NMR ($CDCl_3$): $\delta=195.7$ (C_α), 183.3 (C_γ), 179.9 (C_β), 164.6 ($C_6H_4CMe_2CH_2$), 159.6 (C^a), 159.1 (C^b), 156.4 (C^a), 155.7 (C^b), 152.3 ($C_6H_4CMe_2CH_2$), 150.1 (C^1), 147.5 (C^1), 131.1 (C^8), 124.1 (C^2), 123.8 (C^{10}), 123.2 (C^2), 122.7 (C^9), 121.3 (C^{11}), 119.1 (C^3), 118.5 (C^3), 116.4 ($C_\alpha CO_2CH_2CH_3$), 61.9 ($CO_2CH_2CH_3$), 60.1 ($CO_2CH_2CH_3$), 47.5 (CMe_3), 35.8 ($C_6H_4CMe_2CH_2$), 35.5 (CMe_3), 35.4 ($C_6H_4CMe_2CH_2$), 34.3 (CMe_3), 31.1 (CMe_3), 30.9 (CMe_3), 16.0 ($C_6H_4CMe_2CH_2$), 15.2 ($CO_2CH_2CH_3$), 15.1 ppm ($CO_2CH_2CH_3$); MS (FAB): *m/z*: 765.3 [M^++1]; elemental analysis calcd (%) for $C_{36}H_{47}N_2O_4Ir\cdot 1.5\,C_6H_{14}$ (893.48): C 58.04, H 6.74, N 3.47; found: C 57.84, H 6.74, N 3.45.

Preparation of [Ir(dtbpy)($CH_2CMe_2C_6H_4$){C(CO_2Et)CH(CO_2Et)}(xylNC)] (10): 2,6-Dimethylphenyl isocyanide (8.5 mg, 0.065 mmol) was added to a solution of **9** (50 mg, 0.065 mmol) in CH_2Cl_2 (25 mL) and the mixture was stirred at room temperature overnight. The volatiles were then removed in vacuo and the residue was rinsed with hexane and further recrystallized from CH_2Cl_2/hexane to give red crystals suitable for X-ray diffraction analysis. Yield: 45 mg (77 %); ^{1}H NMR (300 MHz, $CDCl_3$): $\delta=0.77$ (s, 3H; $C_6H_4CMe_2CH_2$), 0.90 (t, $J=7.2$ Hz, 3H; $CO_2CH_2CH_3$), 1.14 (s, 3H; $C_6H_4CMe_2CH_2$), 1.25 (t, $J=6.9$ Hz, 3H; $CO_2CH_2CH_3$), 1.39 (s, 9H; *t*Bu), 1.46 (s, 9H; *t*Bu), 1.84 (d, $J=11.1$ Hz, 1H; $C_6H_4CMe_2CH_2$), 2.01 (d, $J=9.3$ Hz, 1H; $C_6H_4CMe_2CH_2$), 2.10 (s, 6H; *xyl*NC), 3.78–4.15 (m, 4H; $CO_2CH_2CH_3$), 6.09 (s, 1H; C=C*H*CO_2Et), 6.72 (dd, $J=7.2$, 1.5 Hz, 1H; H^4), 6.81 (dt, $J=7.2$, 1.8 Hz, 1H; H^5), 6.86 (t, $J=8.4$ Hz, 2H; *xyl*NC), 6.92 (d, $J=8.4$ Hz, 2H; *xyl*NC), 7.01 (dt, $J=7.2$, 1.8 Hz, 1H; H^6), 7.17 (dd, $J=6.0$, 2.1 Hz, 1H; H^7), 7.49 (dd, $J=5.7$, 2.1 Hz, 1H; H^3), 7.79 (dd, $J=7.2$, 1.5 Hz, 1H; H^3), 8.05 (d, $J=1.5$ Hz, 2H; H^2), 8.11 (d, $J=6.0$ Hz, 1H; H^1), 9.35 ppm (d, $J=6.0$ Hz, 1H; H^1); IR (KBr): $\tilde{\nu}=2099$ cm^{-1} (C≡N); MS (FAB): *m/z*: 896.5 [M^+ +1]; elemental analysis calcd (%) for $C_{45}H_{56}N_3O_4Ir$ (895.39): C 60.38, H 6.31, N 4.69; found: C 60.48, H 6.34, N 4.73.

Preparation of [(Ir(dtbpy)(CH_2CMe_2Ph){κ^2(*C*,*O*)-C(CO_2Et)CH(CO_2Et)})$_2$][BF_4]$_2$ (11): HBF_4 (9 μL of a 54 % solution in Et_2O, 0.065 mmol) was added to a solution of **9** (50 mg, 0.065 mmol) in Et_2O (10 mL) at 0 °C. The mixture was stirred at room temperature for 30 min and then concentrated to dryness. The residue was washed with hexane and Et_2O and recrystallized from CH_2Cl_2/hexane to give orange crystals suitable for X-ray diffraction analysis. Yield: 38 mg (69 %); ^{1}H NMR (300 MHz, $CDCl_3$): $\delta=1.24$ (t, $J=3.3$ Hz, 6H; $CO_2CH_2CH_3$), 1.29 (s, 18H; *t*Bu), 1.34 (s, 18H; *t*Bu), 1.45 (t, $J=3.3$ Hz, 6H; $CO_2CH_2CH_3$), 1.50 (s, 12H; CH_2CMe_2Ph), 2.49 (d, $J=18$ Hz, 2H; CH_2CMe_2Ph), 3.15 (d, $J=$ 17.7 Hz, 2H; CH_2CMe_2Ph), 4.17–4.89 (m, 8H; $CO_2CH_2CH_3$), 6.75 (d, $J=$ 6.3 Hz, 2H; CH_2CMe_2Ph), 7.02 (t, $J=7.5$ Hz, 2H; CH_2CMe_2Ph), 7.07–7.17 (m, 8H; CH_2CMe_2Ph and C=C*H*CO_2Et), 7.26 (d, $J=7.2$ Hz, 2H; H^3), 7.63 (d, $J=5.4$ Hz, 2H; H^3), 7.76 (s, 2H; H^2), 7.95 (s, 2H; H^2), 8.25 (d, $J=6.3$ Hz, 2H; H^1), 8.76 ppm (d, $J=6.0$ Hz, 2H; H^1); ^{19}F{^{1}H} NMR ($CDCl_3$): $\delta=-150.7$ ppm (s); ^{13}C{^{1}H} NMR ($CDCl_3$): $\delta=195.7$ (C_α), 181.9 (C_γ), 162.9 (C_β), 161.7 (C^a), 160.3 (C^b), 155.8 (C^a), 155.5 (C^b), 149.5 (C^1), 149.1 (C^1), 142.1 (CH_2CMe_2Ph), 130.2 ($C_\alpha CO_2CH_2CH_3$), 129.7 (CH_2CMe_2Ph), 126.2 (C^2), 125.3 (C^2), 124.7 (CH_2CMe_2Ph), 122.9 (CH_2CMe_2Ph), 119.4 (C^3), 119.3 (C^3), 67.1 (CMe_3), 60.3 ($CO_2CH_2CH_3$), 51.3 ($CO_2CH_2CH_3$), 39.2 (CMe_3), 36.5 (CH_2CMe_2Ph), 36.2 (CH_2CMe_2Ph), 35.7 (CH_2CMe_2Ph), 31.0 (CMe_3), 30.9 (CMe_3), 30.1 (CH_2CMe_2Ph), 15.0 ($CO_2CH_2CH_3$), 14.6 ppm ($CO_2CH_2CH_3$); MS (FAB): *m/z*: 1531.3 [M^+ +1]; elemental analysis calcd (%) for $C_{72}H_{96}N_4B_2F_8O_8Ir_2\cdot 1.5\,CH_2Cl_2$ (1830.59): C 48.21, H 5.45, N 3.06; found: C 48.09, H 5.76, N 3.04.

X-ray crystallography: Crystal data and experimental details for **2**–**5** and **8**–**11** are summarized in Table 1. Preliminary examinations and intensity data collections were carried out on a Bruker SMART-APEX 1000 area-detector diffractometer using graphite-monochromated $Mo_{K\alpha}$ radiation ($\lambda=0.70173$ Å). The collected frames were processed with SAINT soft-

ware.[38] The data were corrected for absorption using the SADABS program.[39] Structures were solved by direct methods and refined by full-matrix least-squares on F^2 using the SHELXTL software package.[40] Unless stated otherwise, non-hydrogen atoms were refined with anisotropic displacement parameters. Carbon-bonded hydrogen atoms were included in calculated positions and refined in the riding mode using the SHELXL97 default parameters. CCDC-602732 (**2**), CCDC-602733 (**3**), CCDC-602734 (**4**), CCDC-602735 (**5**), CCDC-602736 (**8**·CH_2Cl_2), CCDC-602737 (**9**), CCDC-602738 (**10**), and CCDC-602379 (**11**) contain the supplementary crystallographic data for this paper. These data can be obtained free of charge from the Cambridge Crystallographic Data Centre via www.ccdc.cam.ac.uk/data_request/cif.

Acknowledgements

This work has been supported by the Hong Kong Research Grants Council (project numbers 601705 and HKUST6089/02P). We thank Dr. Herman H. Y. Sung for solving the crystal structures and Mr. Ka-Wang Chan for recording the NMR spectra.

[1] I. M. Dixon, J.-P. Collin, J.-P. Sauvage, L. Flamigni, S. Encinas, F. Barigelletti, *Chem. Soc. Rev.* **2000**, *29*, 385, and references therein.
[2] a) R. J. Watts, S. Efrima, H. Metiu, *J. Am. Chem. Soc.* **1979**, *101*, 2742; b) Y. Ohsawa, S. Sprouse, K. A. King, M. K. DeArmond, K. W. Hanck, R. J. Watts, *J. Phys. Chem.* **1987**, *91*, 1047; c) S. Sprouse, K. A. King, P. J. Spellane, R. J. Watts, *J. Am. Chem. Soc.* **1984**, *106*, 6647; d) F. O. Garces, K. A. King, R. J. Watts, *Inorg. Chem.* **1988**, *27*, 3464.
[3] a) S. Ogo, K. Uehara, T. Abura, Y. Watanabe, S. Fukuzumi, *J. Am. Chem. Soc.* **2004**, *126*, 16520; b) S. Ogo, N. Makihara, Y. Kaneko, Y. Watanabe, *Organometallics* **2001**, *20*, 4903; c) R. Ziessel, *J. Am. Chem. Soc.* **1993**, *115*, 118; d) W. Kaim, R. Reinhardt, M. Sieger, *Inorg. Chem.* **1994**, *33*, 4453.
[4] a) T. Ishiyama, J. Takagi, K. Ishida, N. Miyaura, N. Anastasi, J. F. Hartwig, *J. Am. Chem. Soc.* **2002**, *124*, 390; b) J. Takagi, K. Sato, J. F. Hartwig, T. Ishiyama, N. Miyaura, *Tetrahedron Lett.* **2002**, *43*, 5649; c) T. Ishiyama, J. Takagi, J. F. Hartwig, N. Miyaura, *Angew. Chem.* **2002**, *114*, 3182; *Angew. Chem. Int. Ed.* **2002**, *41*, 3056; d) T. Ishiyama, Y. Nobuta, J. F. Hartwig, N. Miyaura, *Chem. Commun.* **2003**, 2924; e) T. Ishiyama, J. Takagi, Y. Yonekawa, J. F. Hartwig, N. Miyaura, *Adv. Synth. Catal.* **2003**, *345*, 1103; f) K. Kurotobi, M. Miyauchi, K. Takakura, T. Murafuji, Y. Sugihara, *Eur. J. Org. Chem.* **2003**, 3663; g) A. Datta, A. Köllhofer, H. Plenio, *Chem. Commun.* **2004**, 1508; h) D. N. Coventry, A. S. Batsanov, A. E. Goeta, J. A. K. Howard, T. B. Marder, R. N. Perutz, *Chem. Commun.* **2005**, 2172; i) I. A. I. Mkhalid, D. N. Coventry, D. Albesa-Jove, A. S. Batsanov, J. A. K. Howard, R. N. Perutz, T. B. Marder, *Angew. Chem.* **2006**, *118*, 503; *Angew. Chem. Int. Ed.* **2006**, *45*, 489;
[5] a) T. Ishiyama, K. Sato, Y. Nishio, N. Miyaura, *Angew. Chem.* **2003**, *115*, 5504; *Angew. Chem. Int. Ed.* **2003**, *42*, 5346; b) T. Ishiyama, K. Sato, Y. Nishio, T. Saiki, N. Miyaura, *Chem. Commun.* **2005**, 5065.
[6] a) D. Kunz, J. F. Hartwig, C. E. Webster, Y. B. Fan, M. B. Hall, *J. Am. Chem. Soc.* **2003**, *125*, 858; b) T. M. Boller, J. M. Murphy, M. Hapke, T. Ishiyama, N. Miyaura, J. F. Hartwig, *J. Am. Chem. Soc.* **2005**, *127*, 14263.
[7] a) P. N. Nguyen, H. P. Blom, S. A. Westcott, N. J. Taylor, T. B. Marder, *J. Am. Chem. Soc.* **1993**, *115*, 8329; b) J. Y. Cho, M. K. Tse, D. Holmes, R. E. Maleczka, M. R. Smith, *Science* **2002**, *295*, 305.
[8] H. Tamura, H. Yamazaki, H. Sato, S. Sakaki, *J. Am. Chem. Soc.* **2003**, *125*, 16114.
[9] E. C. Constable, J. M. Holmes, *J. Organomet. Chem.* **1986**, *301*, 203.
[10] R. J. Watts, *Inorg. Chem.* **1981**, *20*, 2302.
[11] a) P. K. Byers, A. J. Canty, B. W. Skelton, A. H. White, *Organometallics* **1990**, *9*, 826; b) A. J. Canty, *Acc. Chem. Res.* **1992**, *25*, 83.
[12] a) R. A. Periana, D. J. Taube, S. Gamble, H. Taube, T. Satoh, H. Fuji, *Science* **1998**, *280*, 560; b) S. S. Stahl, J. A. Labinger, J. E. Bercaw, *Angew. Chem.* **1998**, *110*, 2298; *Angew. Chem. Int. Ed.* **1998**, *37*, 2180.
[13] a) D. L. Strout, S. Zarić, S. Q. Niu, M. B. Hall, *J. Am. Chem. Soc.* **1996**, *118*, 6068; b) M.-D. Su, S.-Y. Chu, *J. Am. Chem. Soc.* **1997**, *119*, 5373; c) H. Tamura, H. Yamazaki, H. Sato, S. Sakaki, *J. Am. Chem. Soc.* **2003**, *125*, 16114; d) S. R. Klei, T. D. Tilley, R. G. Bergman, *J. Am. Chem. Soc.* **2000**, *122*, 1816.
[14] a) A. Pedersen, M. Tilset, *Organometallics* **1994**, *13*, 4887; b) P. Diversi, S. Iacoponi, G. Ingrosso, F. Laschi, A. Lucherini, C. Pinzino, G. Uccello-Barretta, P. Zanello, *Organometallics* **1995**, *14*, 3275.
[15] a) K. Isobe, P. M. Bailey, P. M. Maitlis, *J. Chem. Soc. Chem. Commun.* **1981**, 808; b) P. J. Alaimo, R. G. Bergman, *Organometallics* **1999**, *18*, 2707.
[16] a) R. S. Hay-Motherwell, G. Wilkinson, B. Hussain-Bates, M. B. Hursthouse, *Polyhedron* **1991**, *10*, 1457; b) R. S. Hay-Motherwell, G. Wilkinson, B. Hussain-Bates, M. B. Hursthouse, *J. Chem. Soc. Dalton Trans.* **1992**, 3477.
[17] R. S. Hay-Motherwell, G. Wilkinson, B. Hussain-Bates, *Polyhedron* **1993**, *12*, 2009.
[18] a) S. K. Thomson, G. B. Young, *Organometallics* **1989**, *8*, 2068; b) B. C. Ankianiec, V. Christou, D. T. Hardy, S. K. Thomson, G. B. Young, *J. Am. Chem. Soc.* **1994**, *116*, 9963.
[19] a) P. Hofmann, H. Heiss, P. Neiteler, G. Müller, J. Lachmann, *Angew. Chem.* **1990**, *102*, 935; *Angew. Chem. Int. Ed. Engl.* **1990**, *29*, 880; b) L. S. Chang, M. P. Johnson, M. J. Fink, *Organometallics* **1991**, *10*, 1219; c) C. M. Ong, T. J. Burchell, R. J. Puddephatt, *Organometallics* **2004**, *23*, 1493.
[20] T. S. Koloski, P. J. Carroll, D. H. Berry, *J. Am. Chem. Soc.* **1990**, *112*, 6405.
[21] a) K. Itoh, T. Fuakhori, *J. Organomet. Chem.* **1988**, *349*, 227; b) W. Lin, S. R. Wilson, G. S. Girolami, *J. Am. Chem. Soc.* **1993**, *115*, 3022; c) Q. D. Shelby, W. Lin, G. S. Girolami, *Organometallics* **1999**, *18*, 1904.
[22] K. M. Cheung, Q. F. Zhang, K. W. Chan, M. H. W. Lam, I. D. Williams, W. H. Leung, *J. Organomet. Chem.* **2005**, *690*, 2913.
[23] See, for example: T. D. Tilley, in *The Silicon-Heteroatom Bond* (Eds.: S. Patai, Z. Rappoport), Wiley, New York, **1991**, pp. 264 and 343.
[24] J. Cámpora, P. Palma, E. Carmona, *Coord. Chem. Rev.* **1999**, *195*, 207.
[25] a) D. C. Griffiths, B. G. Young, *Organometallics* **1989**, *8*, 875; b) E. Carmona, E. Gutiérrez-Puebla, J. M. Martín, A. Monge, M. Paneque, M. L. Poveda, C. Ruiz, *J. Am. Chem. Soc.* **1989**, *111*, 2883.
[26] J. Cámpora, J. A. López, P. Palma, P. Valerga, E. Spillner, E. Carmona, *Angew. Chem.* **1999**, *111*, 199; *Angew. Chem. Int. Ed.* **1999**, *38*, 147.
[27] J. Cámpora, P. Palma, D. d. Río, E. Carmona, C. Graiff, A. Tiripicchio, *Organometallics* **2003**, *22*, 3345.
[28] R. H. Crabtree, E. M. Holt, M. Lavin, S. M. Morehouse, *Inorg. Chem.* **1985**, *24*, 1986.
[29] J. Cámpora, E. Gutiérrez-Puebla, J. A. López, A. Monge, P. Palma, D. d. Río, E. Carmona, *Angew. Chem.* **2001**, *113*, 3753; *Angew. Chem. Int. Ed.* **2001**, *40*, 3641.
[30] A. B. Tamayo, B. D. Alleyne, P. I. Djurovich, S. Lamansky, I. Tsyba, N. N. Ho, R. Bau, M. E. Thompson, *J. Am. Chem. Soc.* **2003**, *125*, 7377.
[31] K. Onitsuka, H. Urayama, K. Sonogashira, F. Ozawa, *Chem. Lett.* **1995**, 1019.
[32] a) Y. Yamamoto, X.-H. Han, K.-i. Sugawara, S. Nishimura, *Angew. Chem.* **1999**, *111*, 1318; *Angew. Chem. Int. Ed.* **1999**, *38*, 1242; b) Y. Yamamoto, X.-H. Han, S. Nishimura, K.-i. Sugawara, N. Nezu, T. Tanase, *Organometallics* **2001**, *20*, 266.
[33] a) A. M. Clark, C. E. F. Rickard, W. R. Roper, L. J. Wright, *Organometallics* **1999**, *18*, 2813; b) M. K. Lau, Q. F. Zhang, J. L. C. Chim, W.-T. Wong, W.-H. Leung, *Chem. Commun.* **2001**, 1478.
[34] J. R. Bleeke, P. R. New, J. M. B. Blanchard, T. Haile, A. M. Rohde, *Organometallics* **1995**, *14*, 5127.
[35] R. H. Crabtree, X. W. Li, P. Chen, J. W. Faller, *Organometallics* **2005**, *24*, 4810.

[36] T. Dirnberger, H. Werner, *Organometallics* **2005**, *24*, 5123.
[37] a) Y. Alvarado, O. Boutry, E. Gutiérrez, A. Monge, M. C. Nicasio, M. L. Poveda, P. J. Pérez, C. Ruiz, C. Bianchinni, E. Carmona, *Chem. Eur. J.* **1997**, *3*, 860; b) E. Gutiérrez-Puebla, A. Monge, M. C. Nicasio, P. J. Pérez, M. L. Poveda, E. Carmona, *Chem. Eur. J.* **1998**, *4*, 2225; c) E. Carmona, M. Paneque, M. L. Poveda, *Dalton Trans.* **2003**, 4002.
[38] Bruker *SMART and SAINT+*, *Version 6.02a*, Siemens Analytical X-ray Instruments Inc., Madison, Wisconsin, USA, **1998**.
[39] G. M. Sheldrick, *SADABS*, University of Göttingen, Germany, **1997**.
[40] G. M. Sheldrick, *SHELXTL-Plus V5.1 Software Reference Manual*; Bruker AXS Inc., Madison, Wisconsin, USA, **1997**.

Received: April 21, 2006
Published online: September 22, 2006

